AD-A024217

DIRECTIONALLY SOLIDIFIED IN SITU METAL MATRIX COMPOSITES

FINAL REPORT, PART I

PREPARED UNDER
CONTRACT NO. N00019-74-C-0409

for

NAVAL AIR SYSTEMS COMMAND
DEPARTMENT OF THE NAVY
Washington, D.C. 20361

by

G. Haour, F. Mollard, B. Lux,
A. H. Clauer, and I. G. Wright

April, 1976

"APPROVED FOR PUBLIC RELEASE. DISTRIBUTION UNLIMITED"

BATTELLE

Geneva Research Center
7, route de Drize
1227 Carouge-Geneva
SWITZERLAND

Columbus Laboratories
505 King Avenue
Columbus, Ohio 43201
U.S.A.

DISCLAIMER NOTICE

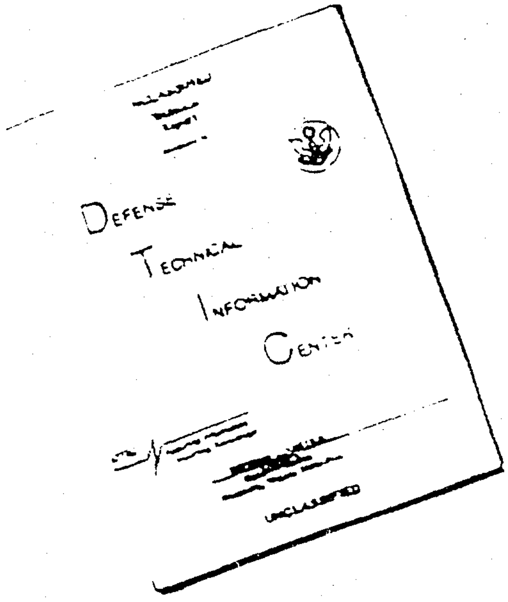

Unclassified

SECURITY CLASSIFICATION OF THIS PAGE (When Data Entered)

REPORT DOCUMENTATION PAGE

READ INSTRUCTIONS BEFORE COMPLETING FORM

1. REPORT NUMBER

2. GOVT ACCESSION NO.

3. RECIPIENT'S CATALOG NUMBER

4. TITLE (and Subtitle)

(6) DIRECTIONALLY SOLIDIFIED IN SITU METAL MATRIX COMPOSITES. Part 1.

NH

5. TYPE OF REPORT & PERIOD COVERED

Final Part 1 (Nov. 1 1974-
Jan. 1, 1976

6. PERFORMING ORG. REPORT NUMBER

7. AUTHOR(s)

(10) G. Haour, F. Mollard, B. Lux, A. H. Clauer [redacted] I. G. Wright

8. CONTRACT OR GRANT NUMBER(s)

(15) N00019-74-C-0409 WEW

9. PERFORMING ORGANIZATION NAME AND ADDRESS

Battelle, Geneva Research Centre, 7 Route de Drize, 1227 Carouge-Geneva, and
505 King Avenue, Columbus, Ohio 432[illegible]1

10. PROGRAM ELEMENT, PROJECT, TASK AREA & WORK UNIT NUMBERS

(16) G6037 (12) 57p.

11. CONTROLLING OFFICE NAME AND ADDRESS

Naval Air Systems Command, Dept. of the Navy,
Washington, D. C. 20361

12. REPORT DATE

(11) Jan [redacted] 76

13. NUMBER OF PAGES

46

14. MONITORING AGENCY NAME & ADDRESS (if different from Controlling Office)

15. SECURITY CLASS. (of this report)

Unclassified

15a. DECLASSIFICATION/DOWNGRADING SCHEDULE

16. DISTRIBUTION STATEMENT (of this Report)

"APPROVED FOR PUBLIC RELEASE. DISTRIBUTION UNLIMITED"

(9) Final rept. 1 Nov 74-1 Jan 76,

17. DISTRIBUTION STATEMENT (of the abstract entered in Block 20, if different from Report)

18. SUPPLEMENTARY NOTES

19. KEY WORDS (Continue on reverse side if necessary and identify by block number)

Eutectics	Ni-Base Alloys
In Situ Composites	Co-Base Alloys
Directional Solidification	Fe-Base Alloys
	Oxidation

20. ABSTRACT (Continue on reverse side if necessary and identify by block number)

The aim of the present alloy screening program was to identify new eutectic superalloys suitable for the manufacture of directionally solidified turbine blades operating at up to 1150 C. In the course of this program, five eutectics not previously investigated have been found to meet the corresponding objectives of a melting point above 1200 C, a

(Continued)

DD FORM 1 JAN 73 1473 EDITION OF 1 NOV 65 IS OBSOLETE

Unclassified

407 080

SECURITY CLASSIFICATION OF THIS PAGE (When Data Entered) specific gravity below 9 g/~~cm^3~~cc and a reasonably low oxidation rate (less than $10^{-7} g^2/cm^4.sec$ at 1150 C).

Their properties are summarized below:

Alloy system	Eutectic temperature (deg. C)	Eutectic composition (wt %)			Oxidation rate at 1150 C in flowing oxygen ($g^2/cm^4.sec$)
Ni-Cr-Ti	1220	54.2	4.6	41.2	10^{-8}
Co-Al-Nb	1240	73.7	3.2	23.1	10^{-7}
Co-Si-Zr	1240	82.5	4.5	13	10^{-7}
Co-Cr-Nb	1280	70.5	18.5	11	6.5×10^{-8}
Co-Cr-Mo	1340	59.9	12.2	27.9	1.3×10^{-8}

These properties are comparable to those of the presently most advanced eutectic superalloys, such as Ni-2.5Al-19.7Nb-6Cr or Co-20TaC-15Cr-8.5Ni-6W. Their oxidation rates, already comparable to that of Co-TaC, measured in the present study, could be further improved by compositional adjustments.

These results were obtained on the basis of a screening of available phase diagrams for 107 alloy systems based on Ni, Co and Fe, from which 52 alloy systems were retained for further study. Twenty-eight simple ternary systems, either not previously evaluated or not described in sufficient detail, were examined experimentally by preparing several samples of compositions close to that determined by a semi-empirical graphical method as closest to the expected eutectic. As a result, 22 eutectics were identified and characterized in terms of melting temperature, microstructure and estimated density. Of these, 10 eutectics were found to meet the objectives of a melting point above 1200 C, a "regular" microstructure presumably amenable to directional solidification and a density below 9 g/~~cm^3~~cc. They were therefore subjected to a systematic investigation of their oxidation resistance, leading to the identification of the 5 promising eutectics previously mentioned.

The remaining 24 alloy systems were not screened because of time and funding constraints.

ABSTRACT

The aim of the present alloy screening program was to identify new eutectic superalloys suitable for the manufacture of directionally solidified turbine blades operating at up to 1150 C. In the course of this program, five eutectics not previously investigated have been found to meet the corresponding objectives of a melting point above 1200 C, a specific gravity below 9 g/cm^3 and a reasonably low oxidation rate (less than 10^{-7}g^2/cm^4.sec at 1150 C).

Their properties are summarized below:

Alloy system	Eutectic temperature (deg. C)	Eutectic composition (w. %)			Oxidation rate at 1150 C in flowing oxygen (g^2/cm^4.sec)
Ni-Cr-Ti	1220	54.2	4.6	41.2	10^{-8}
Co-Al-Nb	1240	73.7	3.2	23.1	10^{-7}
Co-Si-Zr	1240	82.5	4.5	13	10^{-7}
Co-Cr-Nb	1280	70.5	18.5	11	6.5×10^{-8}
Co-Cr-Mo	1340	59.9	12.2	27.9	1.3×10^{-8}

These properties are comparable to those of the presently most advanced eutectic superalloys, such as Ni-2.5Al-19.7Nb-6Cr or Co-20TaC-15Cr-8.5Ni-6W. Their oxidation rates, already comparable to that of Co-TaC, measured in the present study, could be further improved by compositional adjustments.

These results were obtained on the basis of a screening of available phase diagrams for 107 alloy systems based on Ni, Co and Fe, from which 52 alloy systems were retained for further study. Twenty-eight simple ternary systems, either not previously evaluated or not described in sufficient detail, were examined experimentally by preparing several samples of compositions close to that determined by a semi-empirical graphical method as closest to the expected eutectic. As a result, 22

eutectics were identified and characterized in terms of melting temperature, microstructure and estimated density. Of these, 10 eutectics were found to meet the objectives of a melting point above 1200 C, a "regular" microstructure presumably amenable to directional solidification and a density below 9 g/cm^3. They were therefore subjected to a systematic investigation of their oxidation resistance, leading to the identification of the 5 promising eutectics previously mentioned.

The remaining 24 alloy systems are being screened in a continuation of this research effort which will be subsequently reported.

As a result of this study further work is recommended in the following areas:

- investigation of the 24 alloy systems selected but not experimentally studied in the reported study
- improvement of the oxidation resistance of the already identified eutectics by increasing their content in chromium and/or aluminum.
- evaluation of the tensile and creep strength of the five identified eutectics on the basis of directionally solidified samples.
- investigation, using the rapid screening procedure developed in this study, of quasi-ternary systems containing refractory reinforcing phases such as carbides, nitrides and silicides.

TABLE OF CONTENTS

Page

I. INTRODUCTION 1

II. SCOPE OF THE PROGRAM 1

III. APPROACH FOR SCREENING THE ALLOY COMPOSITIONS TO BE PREPARED . 2

III-1 SELECTION OF ALLOY SYSTEMS BASED ON AVAILABLE DATA 2

III-2 SELECTION OF ALLOY COMPOSITIONS TO BE PREPARED FOR THE EXPERIMENTAL SCREENING 5

III-3 EVALUATION OF THE VALIDITY OF THE SEMI-EMPIRICAL SELECTION PROCESS 9

IV. EXPERIMENTAL SCREENING 11

IV-1 PREPARATION OF ALLOY COMPOSITIONS 11

IV-2 MEASUREMENT OF THE EUTECTIC TEMPERATURE 13

IV-3 MEASUREMENT OF THE EUTECTIC COMPOSITIONS 13

IV-4 DENSITY MEASUREMENTS 14

IV-5 OXIDATION STUDIES 14

V. EXPERIMENTAL RESULTS 15

V-1 NICKEL BASE ALLOYS 17

A Ni-Al-Ti 17

B Ni-Al-Zr 17

C Ni-Si-Ti 21

D Ni-Si-V 21

E Ni-Cr-Si 22

F Ni-Cr-Ti 22

G Ni-Cr-Hf 24

H Ni-Cr-Nb 24

I Ni-Nb-B-C and Ni-Mo-B-C 24

V-2 COBALT BASE ALLOYS 27

A Co-Al-Zr 27

B Co-Al-Nb 28

C Co-Al-Ta 28

D Co-C-Zr 28

TABLE OF CONTENTS (Continued)

Page

E Co-Si-Ti 29
F Co-Si-Zr 29
G Co-Si-V 33
H Co-Cr-Si 33
I Co-Cr-Nb 33
J Co-Cr-Mo 35

V-3 IRON-BASE ALLOYS 35
A Fe-Si-Ti 35
B Fe-Si-Zr 37
C Fe-Si-V 37
D Fe-Cr-Ti and Fe-Cr-Zr 37
E Fe-Cr-Ta 40

VI. SUMMARY AND CONCLUSIONS 40

VII. REFERENCES 41

APPENDIX A: LIST OF ALLOY COMPOSITIONS PREPARED IN THE PRESENT ALLOY SCREENING STUDY A-1

APPENDIX B: SUMMARY OF OXIDATION BEHAVIOR AT 1150°C IN 100 mm Hg OXYGEN B-1

LIST OF TABLES

TABLE 1 SCREENING OF Ni-BASE ALLOYS 6

TABLE 2 SCREENING OF Co-BASE ALLOYS 7

TABLE 3 SCREENING OF Fe-BASE ALLOYS 8

TABLE 4 SCREENING OF Ni(Cr)-, Co(Cr)-, Fe(Cr)-BASE ALLOYS INVESTIGATED IN THE PRESENT STUDY 8

TABLE 5 COMPARISON BETWEEN THEORETICALLY PREDICTED AND MEASURED EUTECTIC COMPOSITIONS 9

TABLE 6 SUMMARY OF THE RESULTS OF THE EXPERIMENTAL SCREENING PROGRAM 16

LIST OF FIGURES

Page

FIG. 1 SCHEMATIC REPRESENTATION OF THE THREE CONSTITUENT ALLOY SYSTEMS SCREENED IN THE PRESENT PROGRAM 4

FIG. 2 SELECTION OF ALLOY COMPOSITIONS FOR EXPERIMENTAL SCREENING 10

FIG. 3 SILVER BOAT EQUIPMENT USED TO PREPARE SAMPLES FOR THE EXPERIMENTAL SCREENING 12

FIG. 4 MICROSTRUCTURES OF:
- (a) Ni-5.7Al-19.4Ti 18
- (b) Ni-7.4Al-17.3Zr 18
- (c) Ni-6Si-18Ti 18
- (d) Ni-26Si-4V 18

FIG. 5 OXIDATION KINETICS OF NICKEL-BASE EUTECTICS 19

FIG. 6 CROSS SECTIONS OF OXIDIZED SPECIMENS OF:
- (a) Ni-30Cr 20
- (b) Ni-2.5Al-19.7Nb-6Cr 20
- (c) Ni-6Al-20Ti 20
- (d) Ni-12Al-6Zr 20
- (e) Ni-37Cr-8Si 20
- (f) Ni-4.6Cr-41.2Ti 20

FIG. 7 MICROSTRUCTURES OF:
- (a) Ni-37Cr-8Si 23
- (b) Ni-4.6Cr-41.2Ti 23
- (c) Ni-30.3Cr-8.9Hf 23
- (d) Ni-35Nb-10Cr 23

FIG. 8 CROSS SECTIONS OF OXIDIZED SPECIMENS OF :
- (a) Ni-30.3Cr-8.9Hf 25
- (b) Ni-25Cr-20Nb 25
- (c) Co-35Cr 25
- (d) CoTaC 25
- (e) Co-12.1Al-5.7Zr 25
- (f) Co-30Ti-10Si 25

LIST OF FIGURES (Continued)

Page

FIG. 9 MICROSTRUCTURES OF:
  (a) Ni-18Nb-1.2B-0.8C 26
  (b) Ni-31Mo-2.1B-1.9C 26

FIG. 10 MICROSTRUCTURES OF:
  (a) Co-12Al-5.8Zr 26
  (b) Co-2.7Al-22.5Nb 26

FIG. 11 OXIDATION KINETICS OF COBALT-BASE EUTECTICS 30

FIG. 12 MICROSTRUCTURES OF:
  (a) Co-3.2Al-23.1Nb 31
  (b) Co-0.5Al-32.5Ta 31
  (c) Co-5Si-15Ti 31
  (d) Co-4.5Si-13Zr 31

FIG. 13 CROSS SECTIONS OF OXIDIZED SPECIMENS OF:
  (a) Co-3.2Al-23.1Nb 32
  (b) Co-3.2Al-23.1Nb 32
  (c) Co-4.5Si-13Zr 32
  (d) Co-4.6Si-17.4Zr 32
  (e) Co-40Cr-5Si 32
  (f) Co-18.5Cr-11Nb 32

FIG. 14 MICROSTRUCTURES OF:
  (a) Co-4Si-70V 34
  (b) Co-40Cr-5Si 34
  (c) Co-19.5Cr-25.5Nb 34
  (d) Co-12Cr-28Mo 34

FIG. 15 CROSS SECTIONS OF OXIDIZED SPECIMENS OF:
  (a) Co-12Cr-28Mo 36
  (b) Fe-10Si-22Ti 36
  (c) Fe-5Si-20Zr 36

LIST OF FIGURES (Continued)

Page

FIG. 16 MICROSTRUCTURES OF:

(a) Fe-10Si-22Ti 38

(b) Fe-5Si-20Zr 38

(c) Fe-25Cr-15Ta 38

FIG. 17 OXIDATION KINETICS OF IRON-BASE EUTECTICS 39

DIRECTIONALLY SOLIDIFIED IN SITU
METAL MATRIX COMPOSITES

by

G. Haour, F. Mollard, B. Lux, A. H. Clauer, and I. G. Wright

I. INTRODUCTION

Directional solidification allows the fabrication of gas turbine blades with no grain boundaries perpendicular to the major stress direction, which therefore exhibit superior creep and tensile strength. Furthermore, in directionally-solidifying eutectic superalloys, the aligned phases are finely divided, with no lower melting point components in between. This results in a particularly high bond strength at temperatures close to the eutectic melting point.

The state of the art in the field of directionally solidified eutectics has been reviewed recently at two Conferences on In-Situ Composites held in 1972(1) and 1975(2), respectively. Review papers have also been published by Hogan, et al.(3) as well as Thompson and Lemkey(4). Only a small number of eutectic systems show promise for use as gas turbine blade materials. Among these systems are: Ni-Al-Nb(5,6), Co-TaC(7,8,9), and Ni-TaC(7,8,10).

In the development of these very selectively chosen alloy systems, other eutectics might have been overlooked. For this reason, the present study was aimed at rapidly screening as many alloy systems as possible in an attempt to identify those having potential for use as gas turbine blade materials.

II. SCOPE OF THE PROGRAM

The present program consisted in a wide screening of alloy systems limited to those based on Ni, Co or Fe and containing two reinforcing phases.

The matrix is composed of Ni, Co or Fe, containing in solid solution significant amounts of transition metals, such as Cr, and amounts of non-transitional elements such as Al. The function of Cr or Al would be principally to improve the oxidation characteristics and mechanical properties (by γ'-Ni_3Al strengthening, for example) of the matrix.

The second alloying element would form an intermetallic compound with the matrix as a result of the eutectic reaction. These elements include Ti, Zr, Hf, V, Nb, Ta, Cr, ...

A third constituent is a non-transitional element which forms strong covalent compounds with the matrix. Such elements include, B, Al, C, Si, N and P. These elements have a relatively small solubility in the matrix phase and would be expected to provide a strongly bonded compound phase with high strength and stiffness. Some of them (B, Al, and Si) would be expected to have potential for modifying the scaling characteristics in a beneficial way.

The specific objectives were to identify eutectics not previously investigated having a melting point higher than 1200 C which should in addition, by their oxidation resistance, show promise for use as directionally solidified blades in gas turbines under operating conditions of 1000 hours at 1150 C (2100°F).

They should also exhibit a density not in excess of 9 g/cm^3 and a microstructure making them readily amenable to directional solidification.

III. APPROACH FOR SCREENING THE ALLOY COMPOSITIONS TO BE PREPARED

The approach includes (1) selecting the alloy systems and (2) determining the compositions to be prepared for the experimental screening.

III-1. SELECTION OF ALLOY SYSTEMS BASED ON AVAILABLE DATA

The ternary alloys effectively considered within the scope of the program are schematically illustrated in Fig. 1. Fig. 1a represents 3 matrix elements (Ni, Co, Fe) x 4 non-transitional elements (B, Al, C, Si) x 7 transitional elements (Ti, Zr, Hf, V, Nb, Ta, Cr) = 84 alloy systems, if these elements are taken one by one in each group.

In the course of the evaluation of available data it was found that the Ni-B, Co-B and Fe-B binary eutectics had a melting point too low (about 1100 C) to meet the objectives of this program. The possibility of raising the melting point of the B-containing alloys was explored by introducing that element as a borocarbide. Since compounds such as Mo_2BC have a melting temperature the order of 1800 C, a pseudo-binary eutectic between these compounds and the matrix element could present a desirably high melting point. Two such systems, Ni-Nb-B-C and Ni-Mo-B-C have been retained for experimental investigation in the present study.

Additional alloys having as matrix Ni, Co or Fe with Cr in solution were considered because such a matrix was expected to present an oxidation resistance better than that of a pure metal matrix. These include 21 systems composed of a Ni(Cr), Co(Cr) or Fe(Cr) matrix and one of the following transitional elements: Ti, Zr, Hf, V, Nb, Ta and Mo. They are schematically represented in Fig. 1b.

These simple systems, not containing B, C, Al or Si, were given priority in the investigation. The objectives of the present program would, however, justify further work to investigate more complex (four constituents) alloy systems composed of a matrix, one element chosen among B, C, Al, Si and one among the group: Ti, Zr, Hf, V, Nb, Ta, Mo... The oxidation behavior of the matrix could also be enhanced by using Al; alloys including four constituents (Ni, Co or Fe, Al, + 2 alloying elements) could similarly be considered for investigation. A total of 107 alloy systems have thus been evaluated in the present study. Out of these, alloy systems showing promise and worthy of further experimental investigation have been selected on the basis of the following criteria: (1) the expected eutectic has not been the object of a previous experimental study and (2) only combinations of constituents presenting binary eutectic temperatures higher than about 1250 C were considered in order for the resulting ternary eutectic temperature to be likely to meet the 1200 C objective.

Among the alloy systems meeting these criteria, those having the highest binary eutectic temperatures have, in general, been investigated first. Other considerations, such as expected density and oxidation resis-

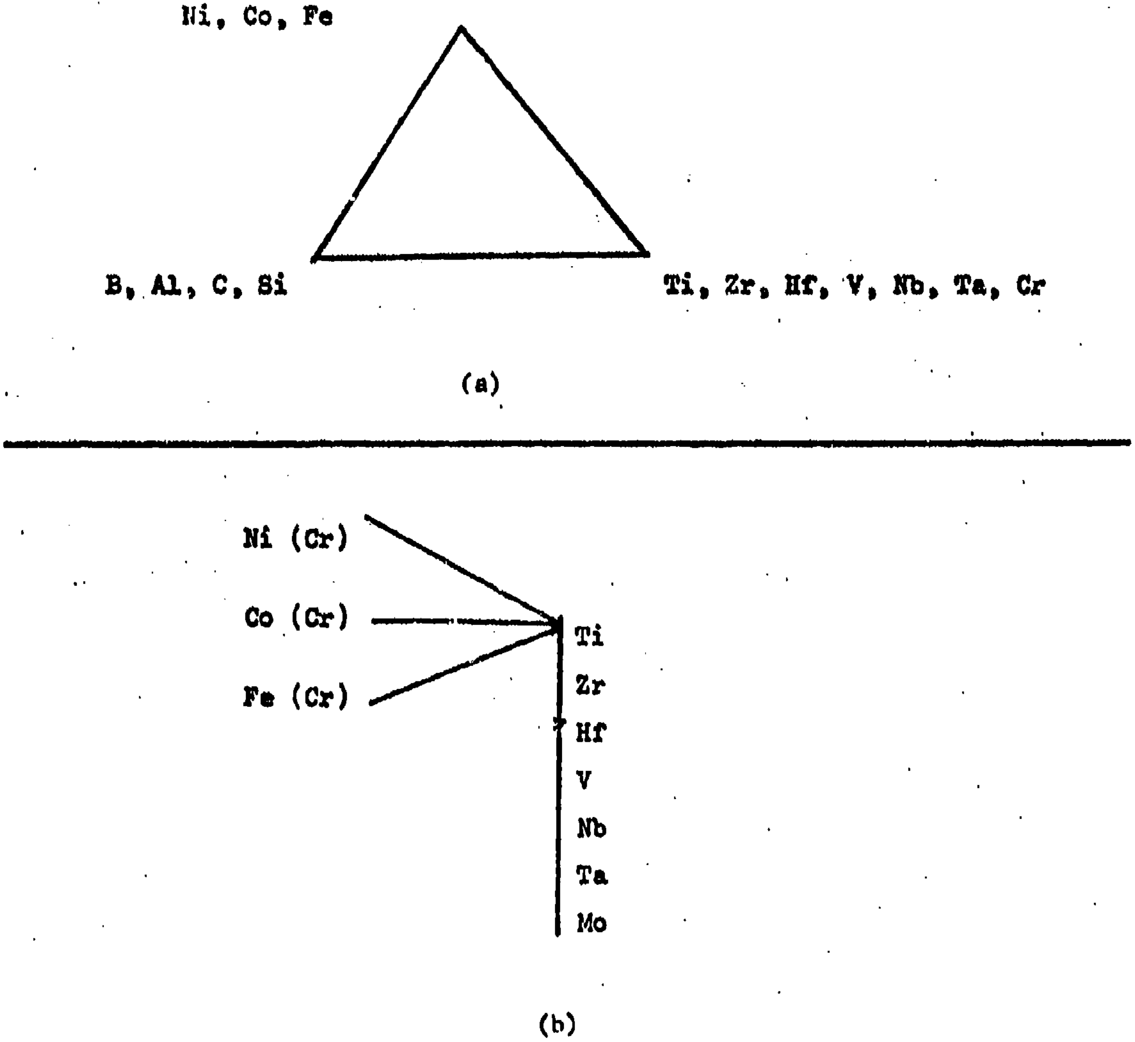

FIG. 1. SCHEMATIC REPRESENTATION OF THE THREE CONSTITUENT ALLOY SYSTEMS SCREENED IN THE PRESENT PROGRAM.

(a) Ni, Co, Fe matrix

(b) Ni(Cr), Co(Cr), Fe(Cr) matrix

tance, have also influenced the order in which the alloy systems have been experimentally examined. Tables 1 to 4 summarise the selection process by indicating the alloy systems not retained after screening and those experimentally investigated in the present study.

In these tables, alloy systems are indicated that had been also retained after the theoretical screening but were not experimentally investigated within the present study for lack of time.

III-2. SELECTION OF ALLOY COMPOSITIONS TO BE PREPARED FOR THE EXPERIMENTAL SCREENING

After having been selected in terms of its expected melting temperature, density and oxidation resistance, each alloy system was experimentally investigated in order to identify a possible eutectic. The paucity of information existing on ternary phase diagrams made it impossible to obtain the exact composition of the ternary eutectic. A rapid semi-empirical method was therefore utilized to determine the approximate composition of the expected eutectic.

Several approaches have been designed in the past in order to provide data on unknown multi-component systems. An empirical approach to the problem has been suggested by Hanak(18) to produce multi-component materials by co-sputtering of their constituents onto a substrate. Computer calculations based on consideration of the structure and the Gibbs free energy of the known binary phases have been made to predict those in the ternary phase diagram(19,20,21). Characteristics of unknown phase diagrams have also been predicted by applying to them patterns evolved from a statistical analysis of thermodynamic data on known systems(22). A recent review article discusses these methods(23).

These tools have been designed to provide knowledge on new phase diagrams and are not advantageously applicable to the present work, because they are either too time consuming or limited by the availability of thermodynamic data, or both.

Since the objective of this program is to rapidly screen as many alloy systems and compositions as possible, an empirical approach making use of the general knowledge of ternary phase diagrams(24) and con-

TABLE 1. SCREENING OF Ni-BASE ALLOYS

Ni	B	Ti	X	Ni-B eutectic temperature (1140) less than 1250 C (Ni-Nb-B-C and Ni-Mo-B-C experimentally investigated in present study)
		Zr		
		Hf		
		V		
		Nb		
		Ta		
		Cr		
	Al	Ti	+	
		Zr	+	
		Hf	x	Al-Hf phase diagram unknown
		V	x	no binary Al-V eutectic
		Nb	x	previously investigated (1, 2, 4, 5, 6)
		Ta	x	previously investigated (11)
		Cr	O	
	C	Ti	x	previously investigated (14)
		Zr	O	
		Hf	x	previously investigated (14)
		V	O	
		Nb	x	previously investigated (14)
		Ta	x	previously investigated (14)
		Cr	x	
	Si	Ti	+	ternary eutectic very rich in Cr (15) expected to be too brittle
		Zr	O	
		Hf	x	
		V	+	
		Nb	O	
		Ta	O	
		Cr	O	

+ : alloy selected and experimentally investigated in the present study

x : not retained for experimental investigation

O : selected alloy not experimentally investigated in the present study

TABLE 2. SCREENING OF Co-BASE ALLOYS

Co	B	Ti	X	Co-B eutectic temperature (1 106 C) less than 1 250 C
		Zr		
		Hf		
		V		
		Nb		
		Ta		
		Cr		
	Al	Ti	o	
		Zr	+	
		Hf	x	Al-Hf phase diagram unknown
		V	x	no Al-V eutectic
		Nb	+	
		Ta	+	
		Cr	O	
	C	Ti	x	previously investigated (14)
		Zr	+	
		Hf	x	previously investigated (14)
		V	x	previously investigated (14)
		Nb	x	previously investigated (14)
		Ta	x	previously investigated (12,13)
		Cr	x	previously investigated (12,13)
	Si	Ti	+	
		Zr	+	
		Hf	o	
		V	+	
		Nb	o	
		Ta	o	
		Cr	+	

\+ : alloy selected and experimentally investigated in the present study

x : not retained for experimental investigation

O : selected alloy not experimentally investigated in the present study

TABLE 3. SCREENING OF Fe-BASE ALLOYS

+ : alloy selected and experimentally investigated in the present study

x : not retained for experimental investigation

o : selected alloy not experimentally investigated in present study

Fe	B		x	Fe-B eutectic temperature (1060 C) less than 1250 C
	Al		x	Fe-Al eutectic temperature (1160 C) less than 1250 C
	C		x	Fe-C eutectic temperature (1153 C) less than 1250 C [Fe-C-Cr previously investigated(1,16)]
	Si	Ti	+	
		Zr	+	
		Hf	o	
		V	+	
		Nb	o	
		Ta	o	

TABLE 4. SCREENING OF Ni(Cr), Co(Cr), Fe(Cr) - BASE ALLOYS INVESTIGATED IN THE PRESENT STUDY

+ : alloy selected and experimentally investigated in the present study

x : not retained for experimental investigation

o : selected alloy not experimentally investigated in the present study

Ni(Cr)	Ti	+	Co(Cr)	Ti	o	Fe(Cr)	Ti	+
	Zr	o		Zr	o		Zr	+
	Hf	+		Hf	o		Hf	o
	V	x no Cr-V eutectic		V	x no Cr-V eutectic		V	x no Cr-V eutectic
	Nb	+		Nb	+		Nb	x previously investigated(17)
	Ta	o		Ta	o		Ta	+
	Mo	o		Mo	+		Mo	o

taining a certain amount of trial and error has been preferred. The choice of a composition likely to be close to the eutectic was made based on a treatment evolved by Hubert(25) for a number of model ternary systems of Co, Sn, Zn, In, and Pb.

According to this treatment, the region most likely to contain a ternary eutectic is the triangle delineated by the three straight lines joining the corners of the concentration diagram to the eutectic composition on the opposite side. This construction is illustrated in Figure 2 for the Co-Cr-Mo alloy system. In the present experimental screening, the first alloy composition to be prepared was that represented by the center of gravity of such a triangle on the ternary phase diagram. This point, corresponding in the above example to 39 Co-45 Cr-16 Mo (in wt %), provided an empirical starting composition in the preparation of samples.

III-3. EVALUATION OF THE VALIDITY OF THE SEMI-EMPIRICAL SELECTION PROCESS

The validity of the treatment(25) used to predict the ternary eutectic composition was evaluated by comparing the ingot composition initially prepared (represented by the center of gravity of the triangle most likely to contain the eutectic) and the actual eutectic composition, as measured by electron-probe microanalysis of the samples.

From such a comparison, it was found that, out of the 10 measured eutectic compositions, 7 of them did lie in the triangle of highest expectancy, as shown below in Table 5.

TABLE 5. COMPARISON BETWEEN THEORETICALLY PREDICTED AND MEASURED EUTECTIC COMPOSITIONS (*INDICATES A MEASURED EUTECTIC COMPOSITION LYING WITHIN THE TRIANGLE OF HIGHEST EXPECTANCY)

Alloy system	Initial alloy composition theoretically close to the eutectic (wt %)			Measured eutectic composition (wt %)		
Ni-Al-Ti	80.5	6.0	13.5	74.0	6.0	20.0
Ni-Cr-Ti	51.0	34.5	14.5	54.2	4.6	41.2*
Ni-Cr-Nb	44.1	42.0	13.9	55.0	25.0	20.0
Co-Al-Nb	75.8	2.5	21.7	73.7	3.2	23.1*
Co-Al-Ta	64.2	4.8	31.0	67.0	0.5	32.5*
Co-Si-Zr	78.1	4.6	17.3	82.5	4.5	13.0*
Co-Cr-Nb	55.1	19.4	25.5	70.5	18.5	11.0
Co-Cr-Mo	39.0	45.1	15.9	59.9	12.2	27.9*
Fe-Si-Ti	68.1	10.1	21.8	77.0	7.0	16.0*
Fe-Si-Zr	74.5	5.1	20.4	77.9	7.9	14.2*

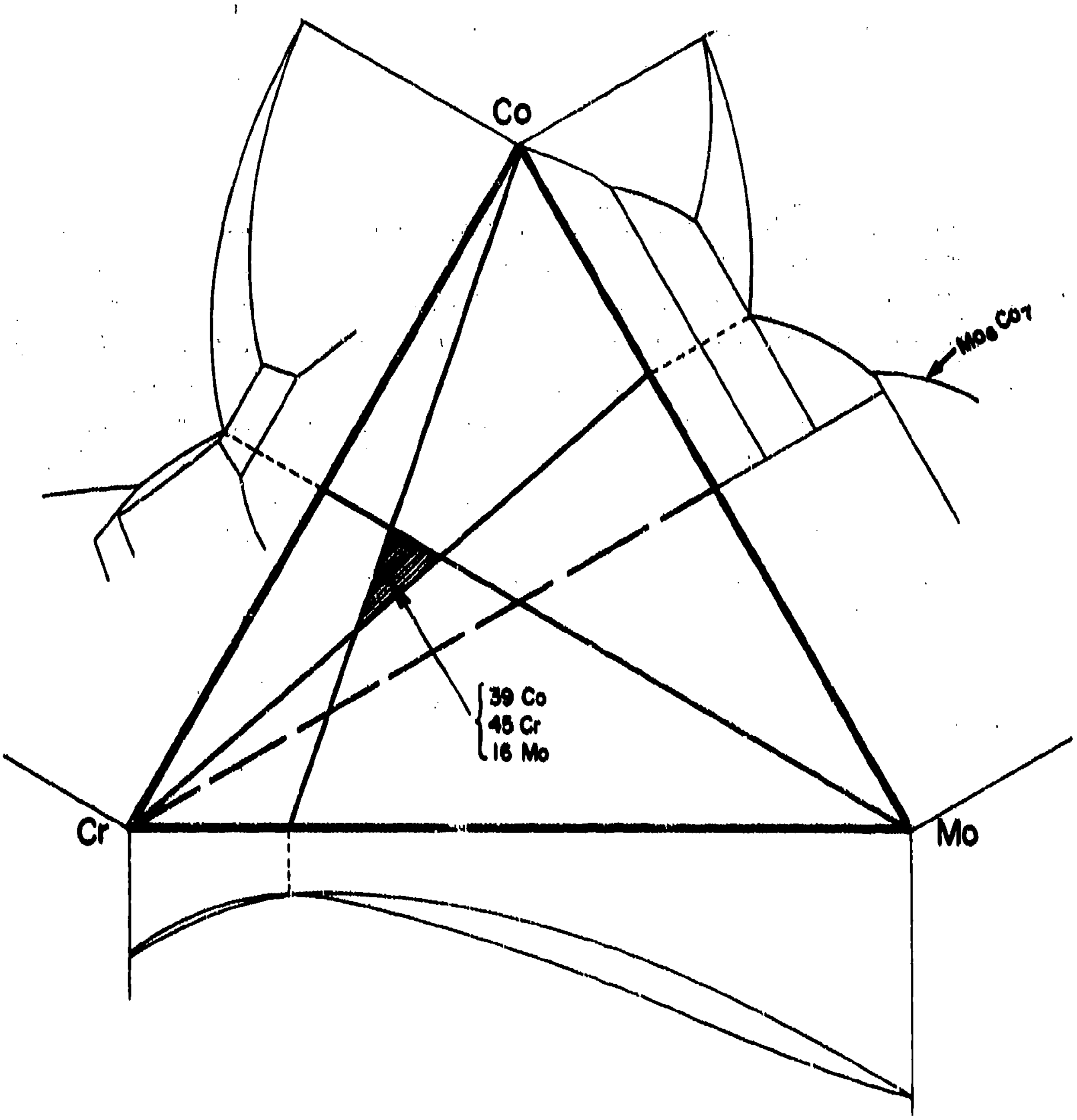

FIGURE 2. SELECTION OF ALLOY COMPOSITIONS FOR EXPERIMENTAL SCREENING. The shaded triangle indicates the area where a ternary eutectic is likely to be found

IV. EXPERIMENTAL SCREENING

The process of identifying and characterizing a eutectic included the following steps: (1) preparation of alloy compositions, (2) measurement of the eutectic temperature and (3) measurement of the eutectic composition. Each of these steps is described below.

IV-1. PREPARATION OF ALLOY COMPOSITIONS

The initial alloy composition to be prepared was derived from the semi-empirical treatment described above.

Samples for screening were prepared using metals of purity 99.97% or better. Appropriate amounts of charge materials were melted in a water-cooled silver boat arrangement shown schematically in Fig. 3. This technique is best suited to produce small ingots from high purity materials without contamination from the crucible. In the set-up utilized, the charge materials were melted and kept melted for a few minutes by induction heating (22 kw at 500 kHz) under a protective argon atmosphere. Residual oxygen contained in the argon was trapped by a heated titanium sponge to further protect the sample from oxidation. The resulting ingot (50 to 80 g, about 6 cm long) was cut into pieces that were placed again in the silver boat and remelted to improve alloying. An average of four successive melting operations was found necessary to achieve sufficient alloying of the charge materials.

The sample of the initial composition was metallographically examined for the presence of a eutectic. If none was observed, additional ingots were prepared to cover a range of compositions within a few percent of the initial composition. This was done in an attempt to detect a eutectic that might have been missed in the initial sample. If, however, none of these samples was shown by metallographic observation to present a eutectic, the investigation of the relevant alloy system was halted. If, on the other hand, the sample initially prepared was observed to contain some eutectic between islands of a primary phase, a second alloy composition was prepared in an attempt to increase the proportion of eutectic. In this new sample, the composition was shifted away from the constituent

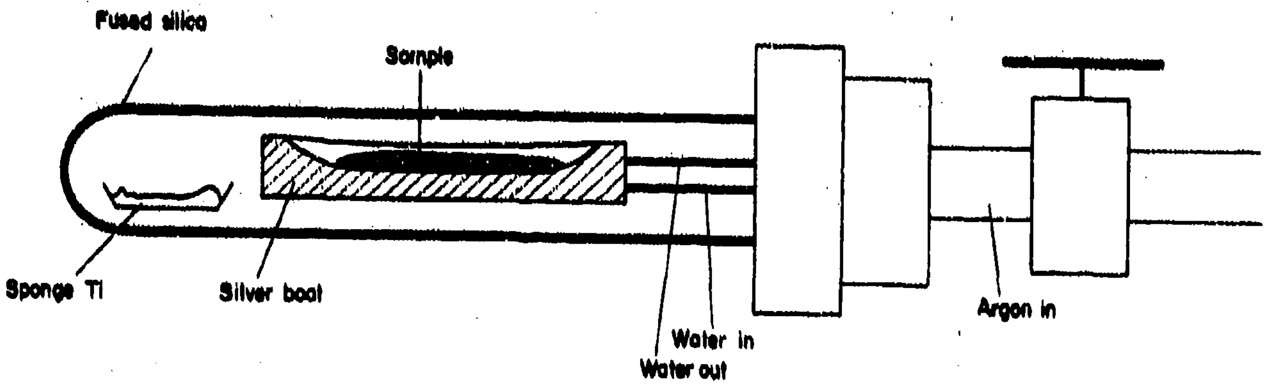

FIG. 3. SILVER BOAT EQUIPMENT USED TO PREPARE SAMPLES FOR THE EXPERIMENTAL SCREENING

of the primary phase. Indications as to the nature of the primary phase were provided by its appearance upon chemical etching. The procedure was repeated until the eutectic represented 20 to 40% of the metallographic section, a proportion sufficient to allow convenient measurement of the eutectic temperature by differential thermal analysis and of the composition by microprobe.

IV-2. MEASUREMENT OF THE EUTECTIC TEMPERATURE

In each sample thus obtained, the eutectic temperatute was measured by differential thermal analysis using a "Linseis" apparatus and Pt/Pt-10 Rh thermocouples. For this, a specimen of about 0.1 cm^3 in volume was placed in a recrystallized alumina crucible.

Heating and cooling of the specimen was carried out under argon at a rate of 6 C/min. The cycle was repeated for each specimen. Temperatures were measured within ± 2C. A eutectic was retained for analysis of its composition if its melting temperature was measured as being not less than 1200 C.

IV-3. MEASUREMENT OF THE EUTECTIC COMPOSITIONS

The composition of a eutectic meeting the melting temperature criterion was then measured by means of an X-ray microprobe attached to a Cambridge Kent "Stereoscan" Scanning Electron Microscope. Measurements were carried out on a wafer about 1 cm x 1 cm cut from the silver boat ingot. On such a specimen, several point counts could be averaged which were obtained by displacing the electron beam within the eutectic. As the size of the beam, about 5 μ, was larger than the thickness of each phase in the eutectic, this technique permitted the overall eutectic composition to be obtained by averaging each composite measurement. The precision thus obtained was such that ingots later prepared on the basis of this determination presented a pure eutectic structure.

This indicated that the accuracy in the analysis was of the same order as that with which the alloy compositions can be prepared in the silver boat, i.e., within 0.2 to 0.5 wt % of the composition sought for, depending on the alloy.

The experimental screening was found to require the preparation of an average of three alloy compositions for each alloy system. The direct analysis on the silver boat sample rendered uneccessary the intermediate step of zone melting to isolate multi-component eutectics(26) envisaged at the beginning of the present program.

IV-4. DENSITY MEASUREMENTS

The eutectic samples cast for the oxidation studies (see below) were also used for density measurements. The latter was derived from the volume of water displaced by a cylinder of known weight, 1/2 cm in diameter, 1 cm long, machined from the cast ingot.

IV-5. OXIDATION STUDIES

The oxidation studies were carried out on 1 cm x 1 cm coupons cut from the silver-boat ingots. Some such ingots were found inappropriate for the measurements, due to the presence of porosity cracks or to their small size. In these cases, additional castings of the alloys were made in an alumina crucible under argon in a Balzers induction furnace of 40 kw power. From the resulting ingot (cylinders about 4 cm high, 3 cm in diameter), 1 cm x 1 cm coupons were cut for the oxidation tests.

The specimens were oxidized isothermally at 1150 C in slowly flowing oxygen under 100 mm Hg pressure in a thermobalance. All specimens were polished through 600 SiC grit papers, 1 μm diamond and 0.03 μm Al_2O_3 paste, and degreased before oxidation. Characterization of the oxidation behavior was by measurement of oxidation kinetics (calculation of the parabolic rate constant, k_p, where applicable), and by optical metallography. The oxidation rates thus measured were compared to three reference alloys: Co-35 Cr ($9.75 \times 10^{-11} g^2/cm^4$.sec.) and Co-10 Cr ($1.11 \times 10^{-7} g^2/cm^4$.sec) for Co-base alloys and to Ni-30Cr ($2.68 \times 10^{-11} g^2/cm^4$.sec.)·) for Ni-base alloys, as well as to two of the eutectic alloys most developed to date: Ni-2.5 Al-19.7 Nb-6 Cr (not parabolic, similar to Ni-30Cr) and Co-20 TaC-15 Cr-8.5 Ni-6 W($1.63 \times 10^{-8} g^2/cm^4$.sec). These five reference alloy systems were tested in the present study on specimens prepared as indicated above, and representative kinetic curves and metallographic cross sections of the scale formed are presented as appropriate in the following sections. A tabulated summary of the oxidation behavior of all alloys tested is presented in Appendix B.

In addition to these detailed oxidation studies, quick preliminary tests of oxidation resistance were performed on Ni-Cr-Nb, Co-Cr-Mo and the three following systems: Ni-Si-V, Co-Si-V and Fe-Si-V, to which the presence of vanadium was expected to confer a poor oxidation behavior. In these tests, the specimens were held at 1150 C in static air for 25 hours. The three V-containing samples were found to have a catastrophic oxidation rate (900 mg/cm^2) compared to Ni-Cr-Nb and Co-Cr-Mo (20 mg/cm^2), reference alloys also studied in the detailed oxidation tests described above.

V. EXPERIMENTAL RESULTS

In the alloys experimentally investigated in the present study, 22 eutectics have been identified. Out of these, 10 eutectics have been investigated to determine their melting temperature, composition, density in some cases, and oxidation resistance. The remaining 12 identified eutectics have not been retained for further consideration because the measured eutectic temperature was below the 1200 C objective (Ni-Al-Zr, Ni-Nb-B-C, Ni-Mo-B-C, Ni(Cu) Mo-B-C, Co-Al-Zr and Co-Si-Ti), or their oxidation behavior proved to be very poor early in the investigation (Ni-Si-V, Co-Si-V and Fe-Si-V); in addition, two eutectics (Ni-Cr-Hf and Fe-Cr-Ta) were expected to have a very high density, estimated to be larger than 10; one eutectic (Co-Cr-Si) was not fully investigated because its divorced microstructure would not be amenable to directional solidification. The alloy compositions prepared are listed in Appendix A of this report. The results obtained in the experimental screening are summarized in Table 6. In the following sections, data are presented for each alloy within the three categories: nickel, cobalt and iron-base alloys.

TABLE 6. SUMMARY OF THE RESULTS OF THE EXPERIMENTAL SCREENING PROGRAM

Alloy system	Eutectic found	Measured eutectic temperature (°C)	Measured eutectic composition (wt%)	Oxidation rate (g^2/cm^4.sec.) (1)
NICKEL-BASE				
Ni-Al-Ti	yes	1305	74.0-6.0-20.0	3.9×10^{-8}
Ni-Al-Zr	yes	1190	(2)	4.65×10^{-9}
Ni-Si-Ti	no	-	-	-
Ni-Si-V	yes	(3)	(3)	poor
Ni-Cr-Si	no	-	-	8.94×10^{-11}
Ni-Cr-Ti	yes	1220	54.2-4.6 - 41.2	$\sim 10^{-8}$
Ni-Cr-Hf	yes	(4)	(4)	5.71×10^{-10}
Ni-Cr-Nb	yes	1190	55.0-25.0-20.0	$\sim 10^{-8}$
Ni-Nb-B-C	yes	1100	(2)	-
Ni-Mo-B-C	yes	1040	(2)	-
Ni(Cu)-Mo-B-C	yes	1130	(2)	-
COBALT-BASE				
Co-Al-Zr	yes	1170	(2)	$\sim 2 \times 10^{-8}$
Co-Al-Nb	yes	1240	73.7-3.2-23.1	$\sim 10^{-7}$
Co-Al-Ta	yes	1290	67.0-0.5-32.5	-
Co-C-Zr	no	-	-	-
Co-Si-Ti	yes	1135	(2)	2.42×10^{-8}
Co-Si-Zr	yes	1240	82.5-4.5-13.0	1.2×10^{-7}
Co-Si-V	yes	(3)	(3)	poor
Co-Cr-Si	yes	(5)	-	2.47×10^{-11}
Co-Cr-Nb	yes	1280	70.5-18.5-11.0	6.47×10^{-8}
Co-Cr-Mo	yes	1340	59.9-12.2-27.9	1.29×10^{-8}
IRON-BASE				
Fe-Si-Ti	yes	1320	76.9-7.2-15.9	1.4×10^{-8}
Fe-Si-Zr	yes	1310	77.9-7.9-14.2	poor
Fe-Si-V	yes	(3)	(3)	poor
Fe-Cr-Ti	no	-	-	-
Fe-Cr-Zr	no	-	-	-
Fe-Cr-Ta	yes	(4)	(4)	poor

(1) An oxidation rate less than that of Co-10 Cr ($10^{-7} g^2/cm^4$.s) is acceptable if no preferential attack of one phase is noted in the sample.

(2) The measured eutectic temperature being inferior to the objective of 1200 C, eutectic composition was not analyzed.

(3) A preliminary test indicated a poor oxidation behavior. No further work was therefore carried out on this eutectic.

(4) A very high density (larger than 10) was expected for this eutectic. No further work was carried out on it as a result.

(5) This eutectic was found to have a divorced structure, therefore not amenable to directional solidification.

V-1. NICKEL-BASE ALLOYS

A. Ni-Al-Ti

In this alloy system, a three-phase Ni_3Al-Ni_2TiAl - Ni_3Ti eutectic of composition 73.9Ni-5.7Al-19.4Ti (in wt %) had been investigated in some detail in a previous study$^{(6)}$. In the present experimental screening, samples were prepared in an attempt to identify a pseudo-binary eutectic expected to occur at 81.6Ni-5.1Al-13.3Ti (in wt %), according to a preliminary study of the Ni_3Al-Ni_3Ti phase diagram$^{(27)}$.

Such samples were, however, found to present a eutectic which, by its microstructure (shown in Fig. 4a) and its measured composition 74 Ni- 6 Al Al-20 Ti (in wt %), turned out to be the three-phase eutectic studied previously.

This eutectic was found to have an oxidation rate of $3.9 \times 10^{-8} g^2/cm^4 \cdot sec$, considerably faster than that of the standard Cr_2O_3-forming alloy Ni-30Cr (Fig. 5). The mode of the oxidation attack is compared to that of Ni-30Cr and the developed eutectic Ni-2.5Al-19.7Nb-6Cr in Figs. 6a to 6c. The simple binary alloy Ni-30Cr forms a uniform, mainly adherent scale of Cr_2O_3, with some grain boundary penetration. Some voids are also visible in the alloy in Fig. 6a, which are possibly Kirkendall voids resulting from the diffusion of chromium from the alloy to the scale. The Ni-Al-Nb-Cr eutectic forms a protective scale which spalls extensively on cooling. Fig. 6b shows only remnants of the external scale, and some preferential internal oxidation of the aligned phase. The oxidation of the Ni-6Al-20Ti alloy was more rapid than that of these other two alloys, but the mode of attack was quite uniform, and therefore predictable, with one phase of the eutectic being preferentially oxidized, as shown in Fig. 6c.

B. Ni-Al-Zr

In a previous investigation$^{(6)}$, a pseudo-binary eutectic Ni_3Al-$NiZr_2$ of composition 75.3Ni-7.4 Al-17.3 Zr had been identified in this alloy system. Some work on this system has been carried out in the

FIG. 4a. Ni-5.7Al-19.4Ti X500
ETCHED, 95H_2O_2-2HF-2HNO_3 (VOL)

FIG. 4b. Ni-7.4Al-17.3Zr X500
ETCHED, 75H_2O-15H_2O_2-10HCL (VOL)

FIG. 4c. Ni-6Si-18Ti X500
ETCHED, 62H_2O-8HNO_3-15H_2SO_4-15HF (VOL)
+ 0.1g$CuSO_4$

FIG. 4d. Ni-26Si-4V X500
ELECTROETCHED, 3% OXALIC ACID

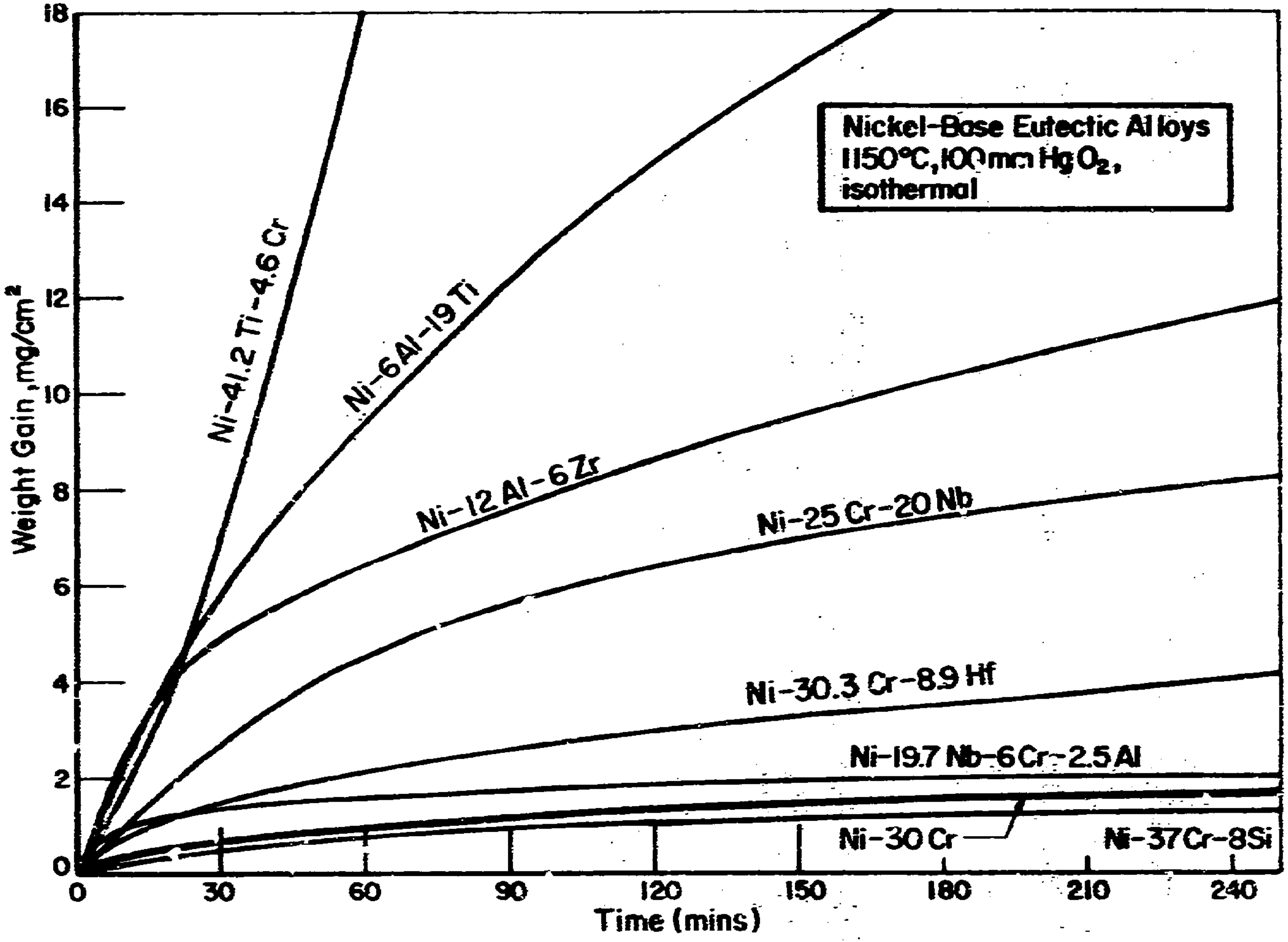

FIG. 5. OXIDATION KINETICS OF NICKEL-BASE EUTECTICS

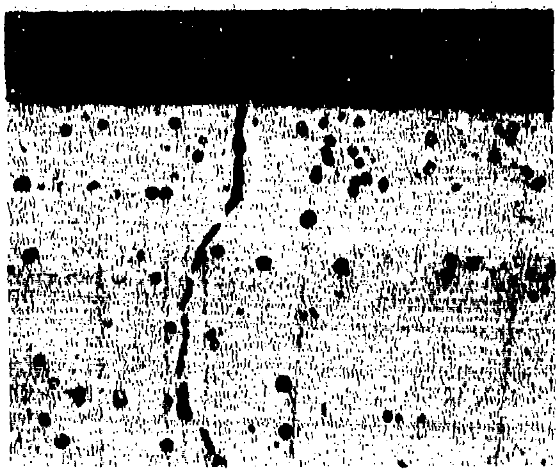

FIG. 6a. Ni-30Cr OXIDIZED 70 hr., X200

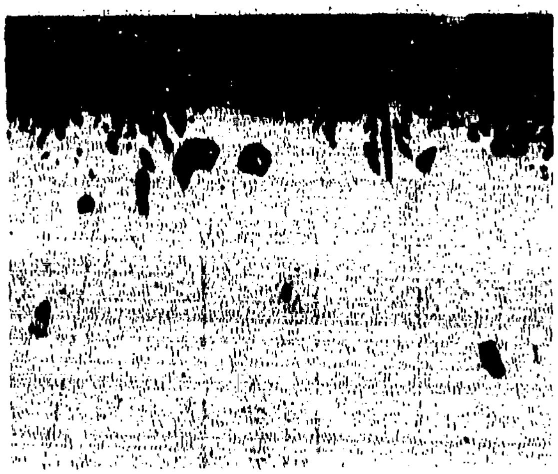

FIG. 6b. Ni-2.5Al-19.7Nb-6Cr OXIDIZED 50 hr., X400

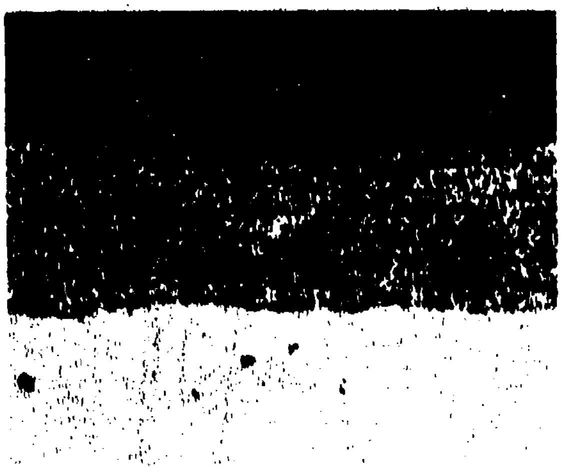

FIG. 6c. Ni-6Al-20Ti OXIDIZED 7.5 hr., X50

FIG. 6d. Ni-12Al-6Zr, OXIDIZED 16.5 hr., X50

FIG. 6e. Ni-37Cr-8Si OXIDIZED 77 hr., X100

FIG. 6f. Ni-4.6Cr-41.2Ti OXIDIZED 2 hr., X100

present study in an attempt to detect a three-phase eutectic. Alloy compositions prepared showed, however, the eutectic (Fig. 4b) mentioned above, between Ni-rich-dendrites.

Its melting point (1190 C), was found to be below the 1200 C objective. No further experimental screening was therefore carried out on this alloy system.

A parabolic rate of 4.65 x $10^{-9}g^{2}/cm^{4}$.sec was, however, determined in oxidation test of a sample of composition Ni-12 Al-6 Zr. This appears to correspond to promising oxidation behavior, Fig. 5, but examination of the microstructure after oxidation showed preferential attack of the eutectic phase with complete penetration of the specimen thickness (0.2 cm) in places after 16.5 hrs. (Fig. 6d).

C. Ni-Si-Ti

In this alloy, the Ni-Si binary phase diagram presents four different eutectics. Only that having the highest Ni Content (88.5 wt%) was considered for the construction on the ternary phase diagram. An initial alloy composition of 16 Ni-6Si-18 Ti and two further compositions were prepared. No eutectic was identified in these samples. In the microstructure of the 76 Ni-6 Si-18 Ti (in wt %) alloy, shown in Fig. 4c, an intermetallic phase appears to undergo a peritectic reaction in the nickel rich matrix.

D. Ni-Si-V

The eutectic identified in this system is shown in Fig. 4d, with some Ni-rich primary phase. As it was expected that the vanadium would cause this system to have poor oxidation resistance, a sample of this alloy was screened in a preliminary oxidation test. It was found that after exposing the sample at 1150 C in static air for 25 hours, the measured weight gain was 900 mg/cm^{2}, making this eutectic inappropriate for the application envisaged. As a consequence, no further work was performed on this system. A similar approach was utilized for the eutectics identified in the Co-Si-V and Fe-Si-V systems (see the following). These systems were also found to have a low oxidation performance.

E. Ni-Cr-Si

No eutectic was observed in the samples of different compositions prepared for the screening of this alloy. A two-phase microstructure, probably Ni_3Si in a Ni (Cr) matrix, was obtained in those samples, as shown in Fig. 7a.

Oxidation testing of a Ni-37 Cr-8 Si alloy indicated a slow oxidation rate (Fig. 5) of 8.94 x $10^{-11} g^2/cm^4.s.$, but a very uneven attack. As shown in Fig. 6e, neither phase was attacked preferentially, and no subsurface attack was noted. The cusp-like irregularities in the oxidized surface were suggestive of attack by a molten phase.

F. Ni-Cr-Ti

In the construction to predict a eutectic in the ternary phase diagram, only the Ni rich (62.5 wt% Ni) eutectic was considered among the 3 eutectics existing in the Ni-Ti binary system.

A eutectic has been thus identified in the course of the experimental screening. Its melting temperature has been measured as being 1220 C. The measured eutectic composition was found to be 54.2 Ni-4.6 Cr-41.2 Ti (in wt %). A sample of that composition was prepared to experimentally confirm this analysis. The resulting microstructure was observed to be composed only of eutectic as shown in Fig. 7b. In this pseudo-binary eutectic, the minor phase, likely to be Ni_3Ti, occupies about 30% of the total volume, in a matrix of Ni (Cr). The melting point (1220 C) is significantly lower than that of Ni_3Al-Ni_3Ti (about 1300 C, as reported in Reference 27) or that of Ni-$_3$Al-Ni_3Nb (1270 C, Reference 6).

Oxidation tests were carried out on a sample of composition 54.2 Ni-4.6Cr-41.2Ti presenting a primary Ni(Cr) phase. Preferential attack of the eutectic phase was noted, at a non-parabolic, rapid rate as shown in Fig. 5. However, the rate of attack tends to slow down and become more uniform in character with time, which may be associated with the development of a zone depleted in eutectic (white zone in Fig. 6f). beneath the band of internal oxide. The Ni-Cr-Ti eutectic appears to offer promising properties in terms of its melting temperature, microstructure, and density, if its oxidation resistance can be improved.

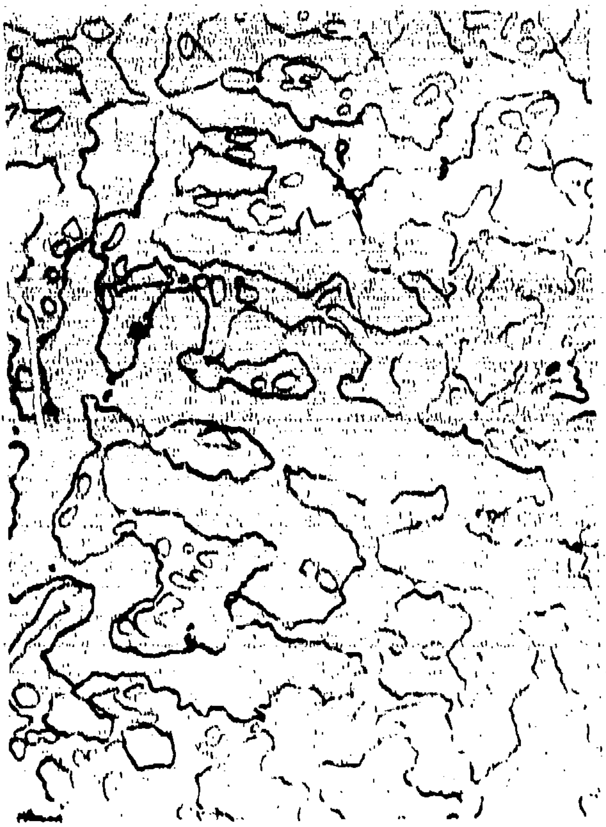

FIG. 7a. Ni-37Cr-8Si X500
ELECTROETCHED, 3% OXALIC ACID

FIG. 7b. Ni-4.6Cr-41.2Ti X1000
ETCHED, $90H_2O$-$5H_2O_2$-5HF (VOL)

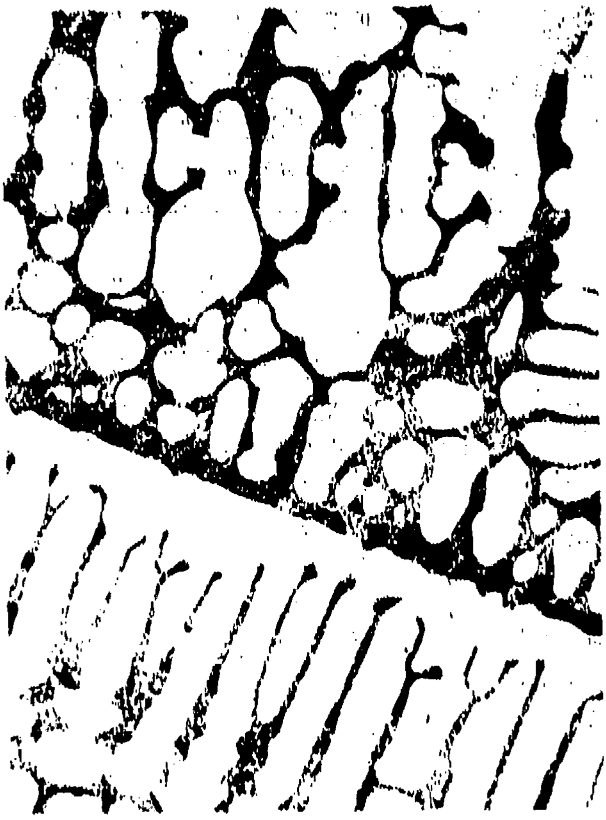

FIG. 7c. Ni-30.3Cr-8.9Hf X500
ETCHED, $62H_2O$-$8HNO_3$-15HF-$15H_2SO_4$ (VOL)

FIG. 7d. Ni-35Nb-10Cr X500
ETCHED, $62H_2O$-$8HNO_3$-$15H_2SO_4$-15HF (VOL)

G. Ni-Cr-Hf

Based on calculations made in a previous study(28), a quasi-binary eutectic reaction has been anticipated in this system to take place at 1317 C for a composition 60.8 Ni-30.3 Cr-8.9 Hf (wt%). A sample having that composition was, however, observed to present only a small portion of eutectic between the Ni(Cr) primary phase, as shown in Fig. 7c. In order to approximate more closely the eutectic composition, Hf contents higher than 15 to 20 wt% Hf were found necessary. Such Hf-levels would raise the alloy specific gravity to calculated values of the order of 10 to 11 g/cm^3. This was thought to be a serious handicap in view of the aeronautical application envisaged so that no further identification of the eutectic was carried out. The oxidation resistance of a 60.8 Ni-30.3 Cr-8.9 Hf (in wt%) was, however, tested indicating a relatively slow rate (Fig. 5), but an extensive internal oxidation of the Hf-rich phase, (Fig. 8a).

H. Ni-Cr-Nb

The Ni-Cr-Nb phase diagram has been reported(29,30) as presenting a pseudo-binary Ni_3Nb-$NbCr_2$ eutectic at a composition of about 55 Ni-35 Nb-10 Cr (wt%). A sample of that composition presented the microstructure shown in Fig. 7d, which shows eutectic between Ni(Cr) dendrites. Further compositions allowed the eutectic to be approximated more closely, so that its chemical composition (55 Ni-25 Cr-20 Nb) and its melting temperature (1190 C) could be measured.

Oxidation tests of a sample very close to the eutectic composition indicated a non-parabolic rate of the order of 10^{-9} g^2/cm^4.s. with extensive internal attack, which appeared as holes rather than internal oxide, which were cusped as if a molten phase had been present (Fig. 8b).

I. Ni-Nb-B-C and Ni-Mo-B-C

The Ni-Nb-B-C system was found to present a eutectic phase, shown between islands of Ni-rich primary phase in Fig. 9a. The eutectic temperature was determined as being 1100 C, too low compared to the objective of 1200 C. No further work was carried out on this system as a result.

FIG. 8a. Ni-30.3Cr-8.9Hf, OXIDIZED 63.5 hr., X50

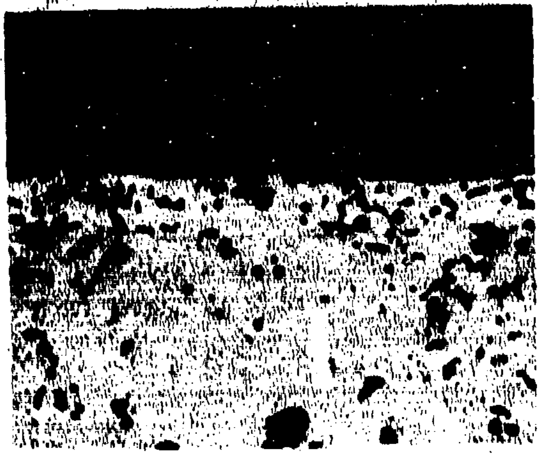

FIG. 8b. Ni-25Cr-20Nb, OXIDIZED 72.5 hr., X200

FIG. 8c. Co-35Cr, OXIDIZED 50 hr., X500

FIG. 8d. CoTaC, OXIDIZED 51 hr., X50

FIG. 8e. Co-12.1Al-5.7Zr, OXIDIZED 20 hr., X50

FIG. 8f. Co-30Ti-10Si, OXIDIZED 9 hr., X50

FIG. 9a. Ni-18Nb-1.2B-0.8C X500
ELECTROETCHED, 3% OXALIC ACID

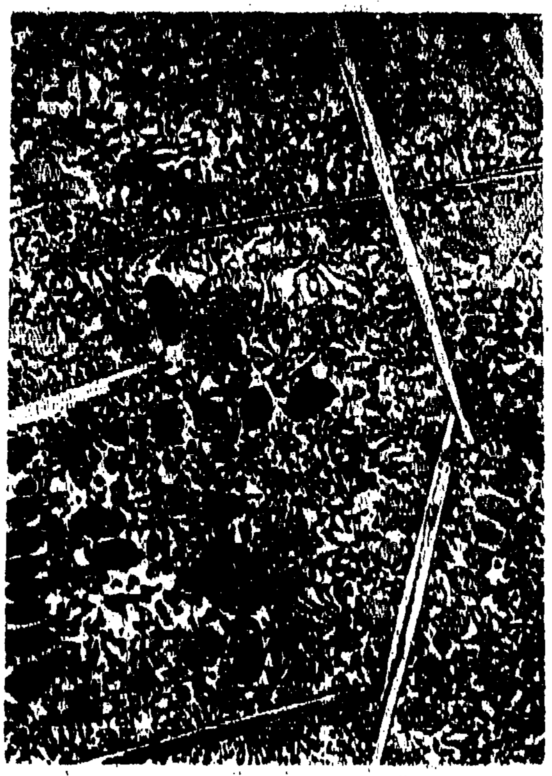

FIG. 9b. Ni-31Mo-2.1B-1.9C X500
ETCHED IN 75H_2O-25H_2O_2-10HCl by VOL.

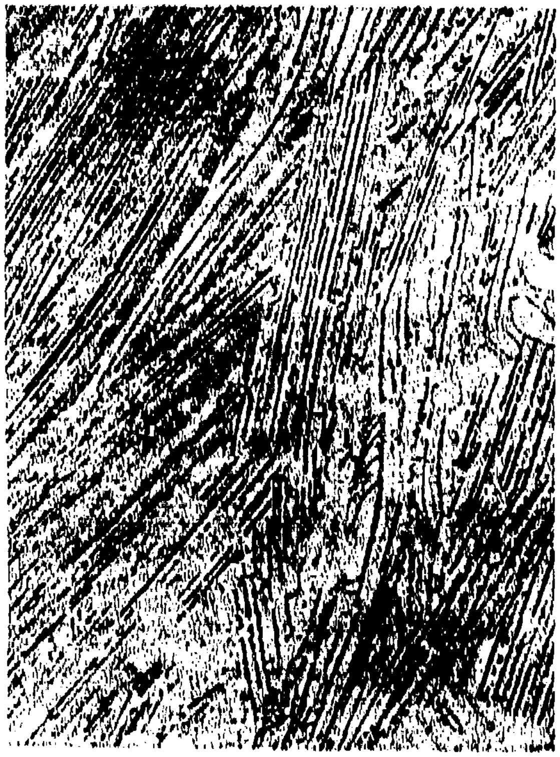

FIG. 10a. Co-12Al-5.8Zr X500
ETCHED, 2%HNO_3 IN ALCOHOL

FIG. 10b. Co-2.7Al-22.5Nb X500
ELECTROETCHED, 3% OXALIC ACID

The Ni-Mo-B-C phase diagram has been studied previously(31,32). Samples of that system prepared for the present investigation were observed to present a eutectic phase. A micrograph illustrating the multiphase structure with needles of borocarbide is shown in Fig. 9b. Small cracks can be seen running through a three-phase structure. The eutectic temperature was measured (1040 C) as being too low for the system to be considered further in the present study. This low melting point is probably due to the higher affinity of boron for nickel than for molybdenum, resulting in the formation of a low melting point Ni-B eutectic. A similar problem would be encountered with analogous systems based on cobalt or iron. Small amounts of copper were added to the Ni-Mo-B-C alloy system, because it considerably decreases the affinity between nickel and boron. This resulted in raising the measured eutectic temperature from 1040 to 1130 C. This still too low temperature, together with the necessity for the copper addition render this system unattractive in view of the application envisaged in the present study. As a consequence no further work was performed on this system.

V-2. COBALT-BASE ALLOYS

A. Co-Al-Zr

In this alloy system a eutectic has been identified with the lamellar structure, shown with some Co-rich primary phase in Fig. 10a. The measured eutectic temperature, 1170 C, was, however, too low for this system to be considered any further. A specimen of the Co-12.1Al-5.7Zr alloy oxidized at a relatively fast, almost parabolic rate ($\sim 2 \times 10^{-8} g^2/cm^4 s$, Fig. 11). Two types of scales were formed, apparently dependent on local variation in the Al or Zr contents. Over most of the specimen, the scale was thin, and blue/purple in color while in a few areas, especially near the specimen edges, the scale was thick, grey, but adherent. Extensive internal oxidation occurred beneath the areas of thin scale, and to a lesser extent below the thick scale (Fig. 8e), indicating very poor oxidation behavior.

B. Co-Al-Nb

A eutectic with the lamellar morphology, shown in Fig. 10b with dendrides of a Co-rich phase has been identified in this system. The eutectic temperature, 1240 C, and the composition, 73.7 Co-3.2 Al-23.1 Nb, have been measured. This result was confirmed by preparing a sample of that composition, which presented an exclusively eutectic structure, as shown in Fig. 12a. The volume fraction of the lamellar phase appears to be 35 to 40%. The density of the eutectic was measured to be $(8.6\pm0.05)g/cm^3$. The eutectic temperature is comparable to that, 1270 C, of the eutectic $Ni-Ni_3Al-Ni_3Nb$(6). The oxidation behavior of a eutectic sample was found acceptable with a uniform attack at a rate comparable to that of a Co-10 Cr alloy (Fig. 11). By oxidizing at a reduced oxygen pressure of 8 mm Hg, the oxidation rate was greatly reduced, to become almost identical to that of the standard Cr_2O_3-forming alloy, Co-35 Cr. The corresponding scale morphologies for oxidation in 100 mm Hg O_2 and 8 mm Hg O_2 are shown in Figs. 13a and 13b. It appears that a small adjustment in composition (probably an increased aluminum content) could significantly improve the oxidation resistance of this alloy. The as yet unknown Co-Al-Nb eutectic thus identified appears promising from the point of view of its microstructure, melting temperature, density and oxidation resistance.

C. Co-Al-Ta

A eutectic identified in this system was found to present the microstructure illustrated in Fig. 12b. Its melting temperature was measured as being 1290 C and its composition as being 67 Co-0.5 Al-32.5 Ta. In the eutectic structure, lamellae are visible between cobalt-rich ($TaCo_2$) dendrites. The high Ta-content of this alloy accounts for the relatively high melting point measured, (1290 C), which should be compared to that (1350 C) of the ternary $Ni-Ni_3Al-Ni_3Ta$ eutectic(11).

D. Co-C-Zr

No eutectic could be identified in this alloy system by experimental screening of 3 samples of compositions: 85 Co-3C-12Zr, 81Co-9C-12Zr and 73Co-9C-18Zr (wt %).

E. Co-Si-Ti

The construction to predict a eutectic on the ternary phase diagram was made relative to the Co-rich (87.5 wt% Co) eutectic among the 4 eutectics existing in the Co-Si binary system. A similar choice was made for the alloys containing Co and Si, i.e.: Co-Si-Zr, Co-Si-V, Co-Cr-Si (see below).

A eutectic has thus been identified. Its structure is shown in Fig. 12c. The measured eutectic temperature, 1135 C, is below the 1200 C objective, so that no further work was carried out in the screening of this alloy system. The oxidation rate of a sample close to the eutectic composition was measured as being $2.4 \times 10^{-8} g^2/cm^4$.sec (Fig. 11). Selective oxidation of one phase and internal porosity led to a very complex oxide structure, shown in Fig. 8f, which would seem to make the alloy unsuitable.

F. Co-Si-Zr

In the course of the present experimental screening, a eutectic was identified in this system with a measured melting temperature of 1240 C. The eutectic composition was analyzed as being 82.5Co-4.5Si-13Zr. A sample prepared with this composition showed the regular lamellar eutectic structure illustrated in Fig. 12d. The density of the eutectic was measured as being $8.10 \pm 0.05 g/cm^3$.

Oxidation tests were carried out using a specially cast eutectic ingot. The rate measured for that sample was $1.2 \times 10^{-7} g^2/cm^4$.s. Preferential oxidation of one of the eutectic phases took place, leading to a relatively uniform layer of internal oxide as shown in Fig. 13c. In contrast, a Co-4.6Si-17.4Zr alloy oxidized at a slower rate of $7.74 \times 10^{-9} g^2/Cm^4$.sec (Fig. 11). Areas free of eutectic were present in this alloy, and these formed uniformly thick, adherent CoO-type scale with no subscale, whereas the eutectic-containing areas formed a thin, grey scale, and a subscale of internal oxide resulting from preferential attack of the eutectic (Fig. 13d). The apparently beneficial effect of an increase in zirconium content from 13 to 17.4% is therefore thought to be related to

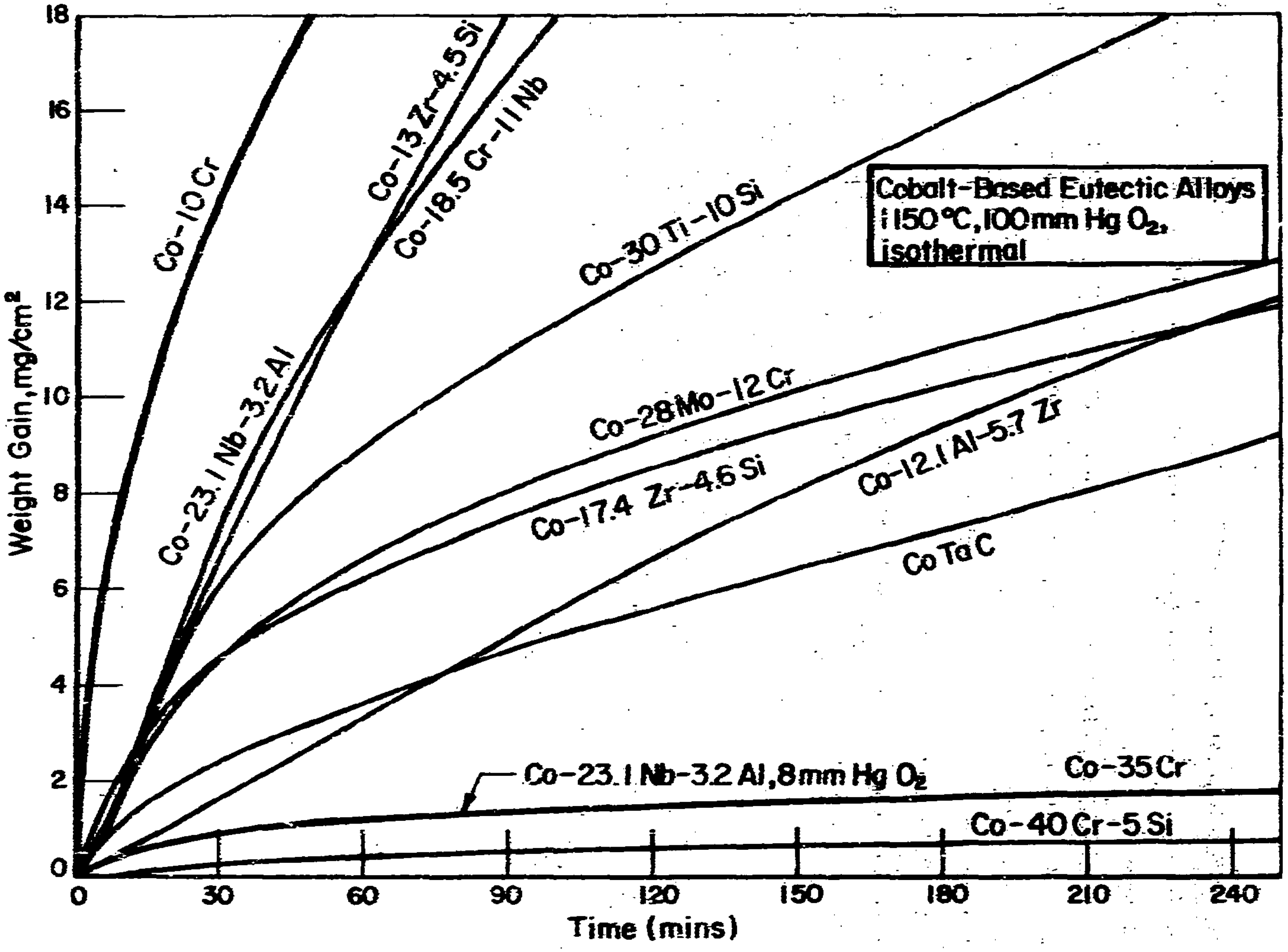

FIG. 11. OXIDATION KINETICS OF COBALT-BASE EUTECTICS

FIG. 12a. Co-3.2Al-23.1Nb X500
ELECTROETCHED, 3% OXALIC ACID

FIG. 12b. Co-0.5Al-32.5Ta X500
ELECTROETCHED, 3% OXALIC ACID

FIG 12c. Co-5Si-15Ti X1000
ELECTROETCHED, 3% OXALIC ACID

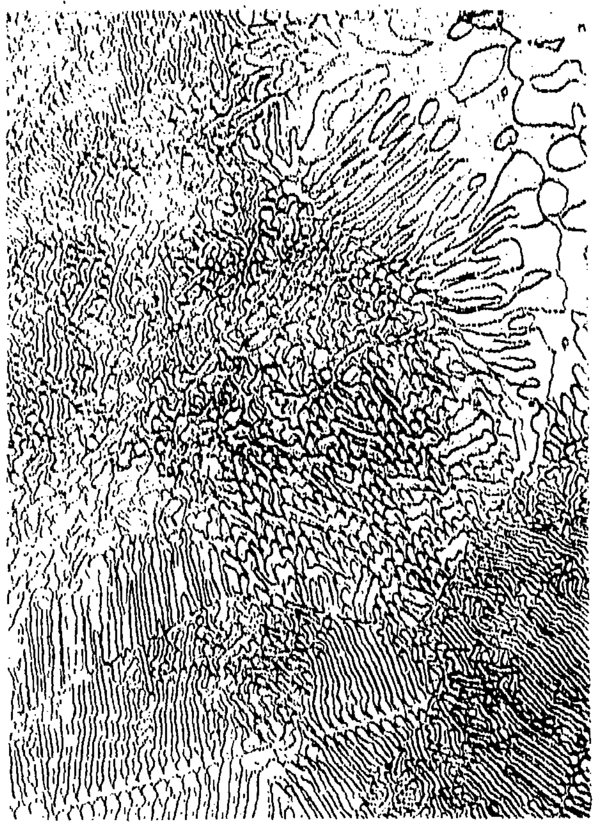

FIG. 12d. Co-4.5Si-13Zr X500
ETCHED, $96H_2O-2HF-2HNO_3$ BY VOL.

FIG. 13a. Co-3.2Al-23.1Nb, OXIDIZED AT 100 mm Hg O_2, X200

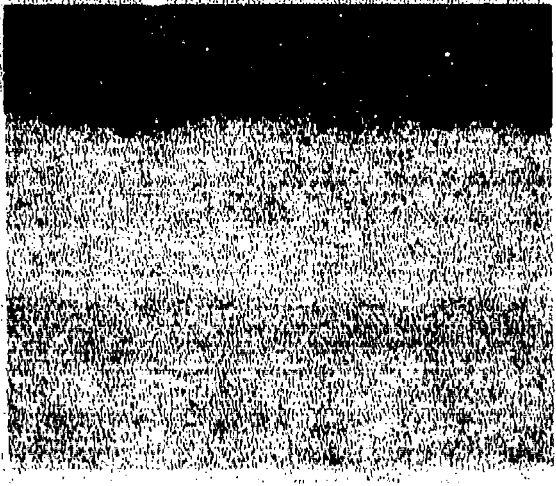

FIG. 13b. Co-3.2Al-23.1Nb, OXIDIZED 2 hrs. AT 8 mm Hg O_2, X200

FIG. 13c. Co-4.5Si-13Zr, OXIDIZED 3.5 hrs., X250

FIG. 13d. Co-4.6Si-17.4Zr, OXIDIZED 3 hr., X200

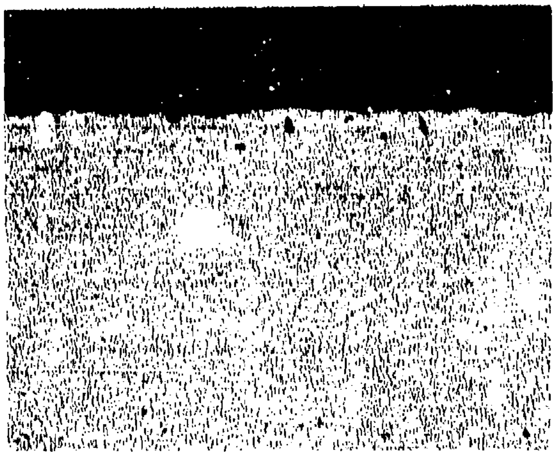

FIG. 13e. Co-40Cr-5Si, OXIDIZED 18 hrs., X200

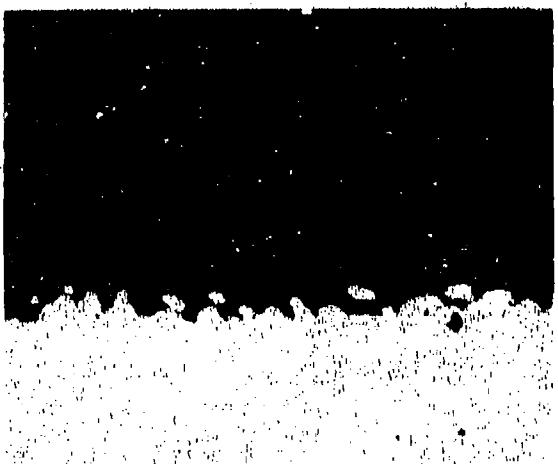

FIG 13f. Co-18.5Cr-11Nb, OXIDIZED 5.5 hr., X100

these differences in alloy microstructure rather than to increased zirconium content per se. This as yet unknown eutectic identified in Co-Si-Zr appears promising from the point of view of its microstructure, melting temperature, density and oxidation resistance.

G. Co-Si-V

The eutectic identified in the screening of this alloy is shown in Fig. 14a, with some Co-rich primary phase. Its microstructure is similar to that of Ni-Si-V. A preliminary test established that the oxidation (800 mg/cm^2 weight gain after 25 hrs at 1150 C in static air) of this alloy was catastrophic, as was the case for Ni-Si-V, due to the presence of vanadium. No further work was therefore performed on this system.

H. Co-Cr-Si

The eutectic identified in this system appears to have a divorced microstructure shown between Co(Cr) dendrites in Fig. 14b, making this eutectic not amenable to directional solidification. No experimental screening was therefore carried out as a result.

The oxidation rate of a sample close to the eutectic composition was found to be slow, $2.47 \times 10^{-11} g^2/cm^4$.sec (Fig. 11) with grain boundary penetration which was very limited after 18 hrs exposure, Fig. 13e, but which was extensive after 77 hrs. The scale on this alloy spalled almost completely on cooling.

I. Co-Cr-Nb

A eutectic phase has been identified in this alloy system in the course of the present investigation. Its lamellar microstructure is shown in Fig. 14c, between dendrites of a Co-rich primary phase. The eutectic melting temperature, 1280 C, and composition, 70.5 Co-18.5 Cr-11 Nb, have been measured. Compared to the eutectic identified in Ni-Cr-Nb (see above), the present eutectic has a much higher melting temperature (1280 against 1190) and is richer in the matrix element (70.5 Co against 54 Ni). The specific gravity of the Co-Cr-Nb eutectic was measured as being 8.50±0.05 g/cm^3.

FIG. 14a. Co-4Si-70V X500
ELECTROETCHED, 3% OXALIC ACID

FIG. 14b. Co-40Cr-5Si X500
ELECTROETCHED, 3% OXALIC ACID

FIG. 14c. Co-19.5Cr-25.5Nb X500
ELECTROETCHED, 3% OXALIC ACID

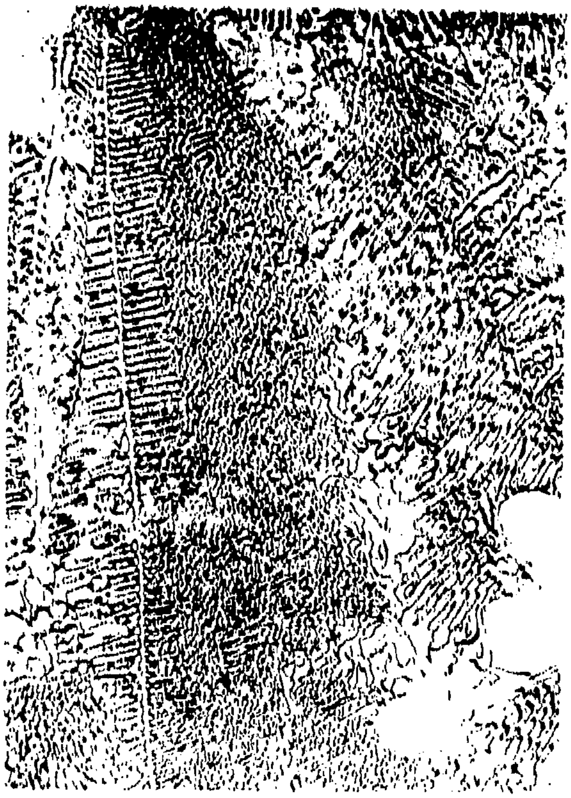

FIG. 14d. Co-12Cr-28Mo X500
ELECTROETCHED, 3% OXALIC ACID

In oxidation tests, the Co-Cr-Nb eutectic was observed to undergo a uniform attack with only slight preferential oxidation, at a parabolic rate of 6.47 x $10^{-8}g^2/cm^4$.sec. (see Fig. 11). The form of the oxidation atack is very similar to that of the developed alloy CoTaC (Fig. 13f). The reason for the difference in oxidation rates between this alloy and CoTaC are not evident without further investigation.

This identified eutectic is therefore promising by its microstructure, melting temperature, density and oxidation resistance.

J. Co-Cr-Mo

Measurements of melting temperature, 1340 C, and composition, Co-12.2 Cr-27.9 Mo, have been made on the eutectic identified in this system by the present study. A special casting prepared on the basis of the measured eutectic composition presented the lamellar microstructure shown in Fig. 14d. It appears to be characteristic of a pseudo-binary eutectic, composed of a Mo_3Co phase in a Co(Cr) matrix. The density of the eutectic was found as being relatively high, 8.9±0.1, due to the high content in molybdenum. A sample of eutectic composition was shown to have a good oxidation behavior with a uniform attack at the relatively fast parabolic rate, of 1.29 x $10^{-8}g^2/cm^4$sec, (Fig. 11). The dark green-blue scale formed on this alloy spalled extensively in cooling, but appeared to be single-layered (Fig. 15a) unlike that formed on a Co-10Cr alloy.

The eutectic identified in the Co-Cr-Mo alloy system appears therefore very promising by its structure, melting temperature and oxidation behavior.

V-3. IRON-BASE ALLOYS

A. Fe-Si-Ti

A eutectic identified in this system was found to have a melting temperature of 1320 C and a composition of 76.9 Fe-7.2 Si-15.9 Ti. The eutectic microstructure, shown in Fig. 16a, probably includes a silicide such as Fe_3Si_3.

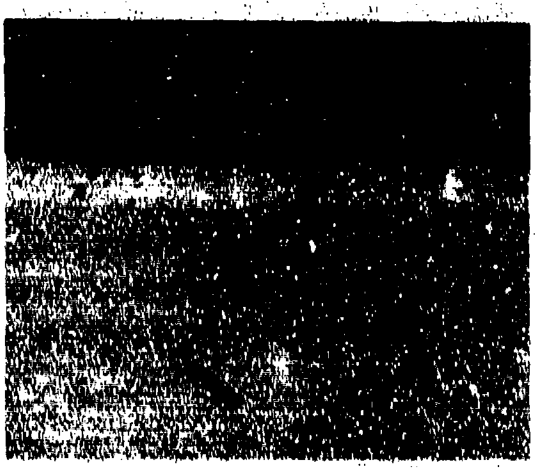

FIG. 15a. Co-12Cr-28[illegible], OXIDIZED
3.5 hr., X500

FIG. 15b. Fe-10Si-22Ti, OXIDIZED
3.5 hr., X100

FIG. 15c. Fe-5Si-20Zr, OXIDIZED
40 min., X50

Oxidation tests have been performed on a sample of composition Fe-10 Si-22 Ti, fairly far removed from the eutectic. A relatively fast but acceptable parabolic rate of about 1.4 x $10^{-8} g^2/cm^4$.sec. was measured for this sample (Fig. 17). The external scale completely spalled on cooling. Fig. 15b shows the morphology of the remaining subscale, and some cracks which developed in the white-appearing Si- and Ti-denuded zone at the alloy surface.

B. Fe-Si-Zr

The present experimental screening has permitted the identification of a eutectic in this alloy. The eutectic composition has been measured to be 77.9 Fe-7.9Si-14.2Zr(wt%). Its microstructure, together with Fe-rich dendrites, is shown in Fig. 16b. Both composition and structure are comparable to those of the Fe-Si-Ti eutectic described above. The melting temperature has been measured in the Fe-Si-Zr eutectic as being 1310 C.

The investigation of the oxidation behavior of a Fe-5Si-20Zr sample indicated that catastrophic oxidation (Fig. 17) initiated after only about 20 minutes of exposure. The rapid attack appeared to be associated with the oxidation of inhomogeneities, possibly Zr-rich, in the alloy (Fig. 15c). The oxidation behavior of the eutectic areas of the specimens appeared uniform and not excessively rapid.

C. Fe-Si-V

The present work revealed the existence of a eutectic in this system. In view of the presence of vanadium in this alloy, its oxidation behavior was expected to be very poor. As a consequence, a rapid oxidation test was performed on a sample close to the eutectic composition, as was done for Ni-Si-V and Co-Si-V. A comparably low oxidation resistance (800 mg/cm^2 weight gain after 25 hrs at 1150 C in static air) was found. No further work was performed on this system as a result.

D. Fe-Cr-Ti and Fe-Cr-Zr

No eutectic has been found in either of these systems after experimental screening of a range of compositions.

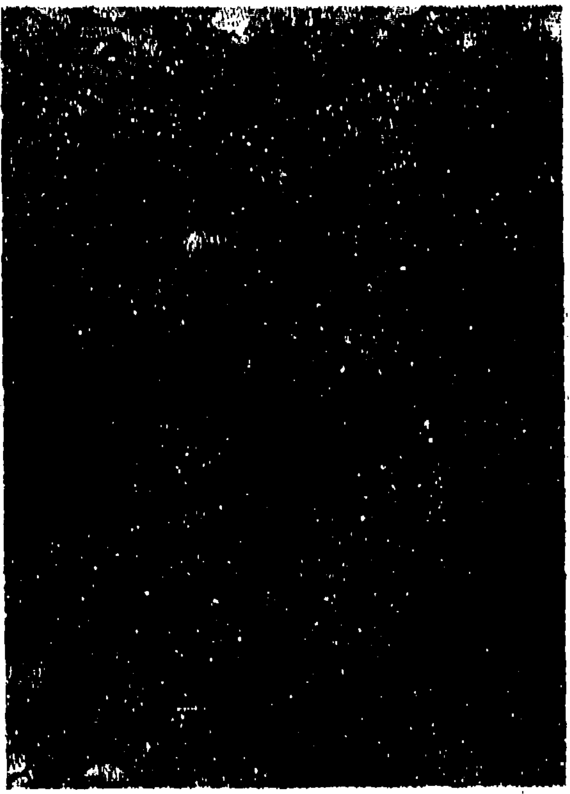

FIG. 16a. Fe-10Si-22Ti X500
ETCHED, 2% HNO_3 IN ALCOHOL

FIG. 16b. Fe-5Si-20Zr X500
ETCHED, 2% HNO_3 IN ALCOHOL

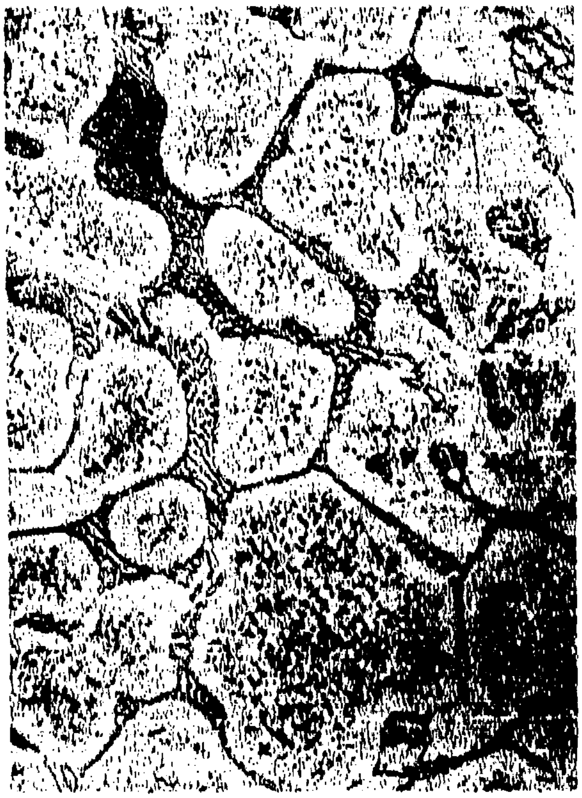

FIG. 16c. Fe-25Cr-15Ta X500
ELECTROETCHED, 3% OXALIC ACID

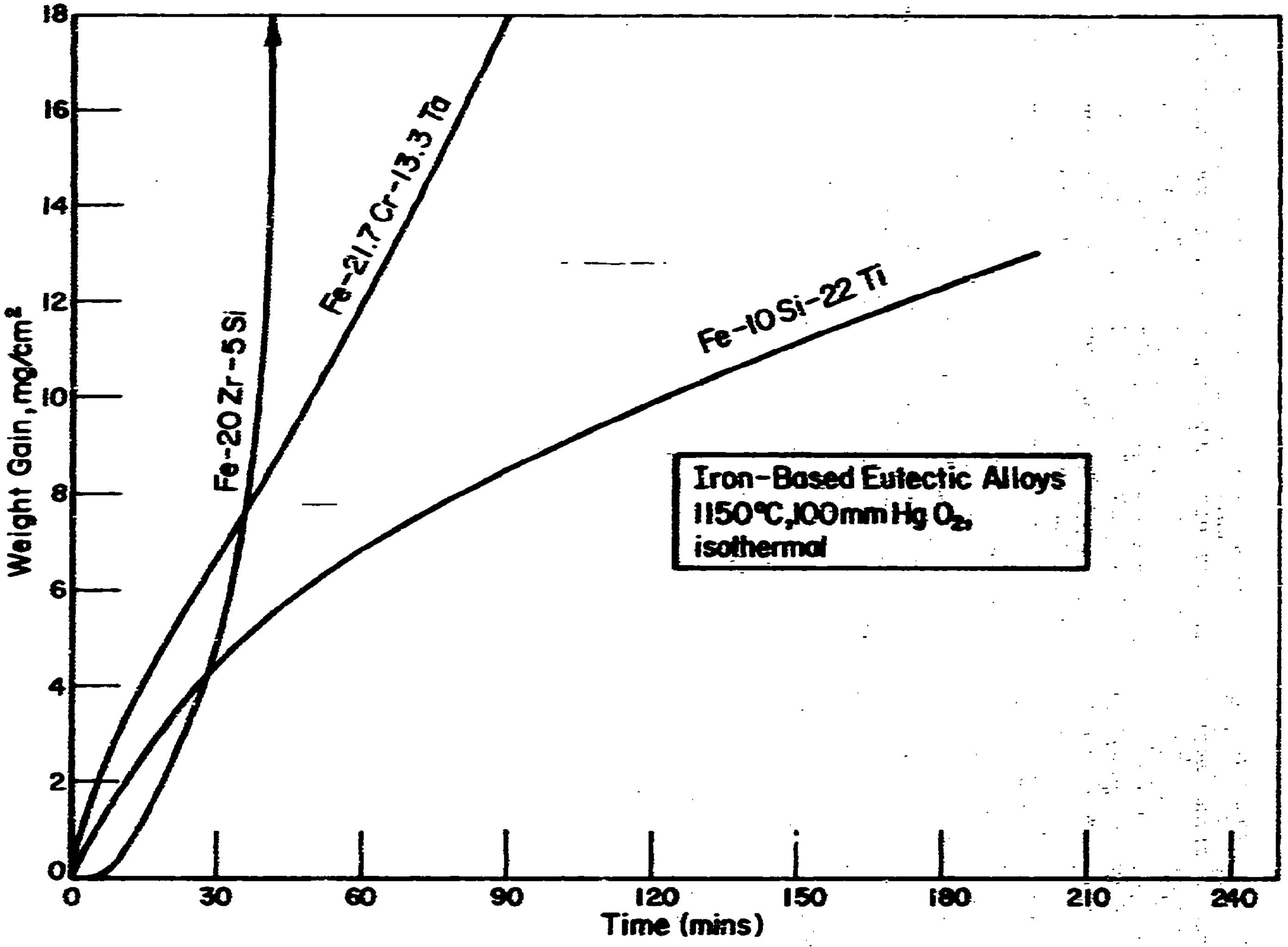

FIG. 17. OXIDATION KINETICS OF IRON-BASE EUTECTICS

E. Fe-Cr-Ta

A eutectic phase in Fe-Cr-Ta has been identified in the course of the present investigation. A sample of composition 60 Fe-25Cr-15Ta (in wt %) is shown in Fig. 16c. It appears to be composed of an iron-rich primary phase separated by eutectic. As this eutectic was, however, expected to contain over 30 wt % Ta and thus have a high density (10 to 11), no further measurement was undertaken on the eutectic.

The oxidation resistance of a sample in this system having the composition (Fe-21.7-Cr-13.3Ta) has been investigated. The specimens used were not homogeneous, and the rapid oxidation rate indicated in Fig. 17 resulted from either the rapid, complete oxidation, or the melting, of a large inclusion of unknown composition. No obvious low melting phases are apparent in the available Fe-Ta or Cr-Ta phase diagrams.

VI. SUMMARY AND CONCLUSIONS

In this program, 107 alloy systems containing Ni, Co or Fe as matrix and two other constituents, have been evaluated on the basis of the available data. 52 of those have been selected for experimental screening, out of which 28 alloy systems could be investigated experimentally. Twenty-two eutectics were then identified, out of which 5 as yet not investigated eutectics were found to have potential for use in gas turbine blades.

These eutectics are:

Alloy	Eutectic temperature (C)	Eutectic composition (wt %)	Oxidation rate at 1150 C in 100 mm Hg O_2 (g^2/cm^4.s.)
Ni-Cr-Ti	1220	54.2-4.6-41.2	10^{-8}
Co-Al-Nb	1240	73.7-3.2-23.1	10^{-7}
Co-Si-Zr	1240	82.5-4.5-13	10^{-7}
Co-Cr-Nb	1280	70.5-18.5-11	6.5×10^{-8}
Co-Cr-Mo	1340	59.9-12.2-27.9	1.3×10^{-8}

These eutectics were found to present a microstructure amenable to directional solidification. Their melting point meets the 1200 C objectives, as they are in fact all above 1220 C. Their measured oxidation behavior, already comparable to the advanced alloy Co-20TaC-15Cr-8.5Ni-6W (wt%), could still be significantly improved by compositional adjustment, such as higher Al contents in the Co-Al-Nb alloy and by optimized Cr levels in the other alloys.

Further work, using the same experimental approach, should be carried out to complete the present research program within its initial scope and objectives in order to identify additional new systems. The screening should be focused on the 24 alloy systems selected but not experimentally investigated in the present study for lack of time. Further systems should also be screened, based on a Ni or Co matrix reinforced by a hardening phase, such as Ni_3Al, and a refractory compound, such as carbides (Ta-C, Ti-C, Mo-C, Zr-C...), nitrides (Ta-N, Ti-N,...), silicides (Ta-Si, Nb-Si, Ti-Si,...) and mixed compounds, such as carbosilicides for example. Recent work in this area(33) has shown that such systems have merits for the application considered.

VII. REFERENCES

(1) Proceedings of the First Conference on In-Situ Composites, 3 vol. (Lakeville, N.Y., U.S.A., 1972), Publication NMAB 308 (Washington, 1973).

(2) Proceedings of the Second Conference on In-Situ Composites (Lake George, N.Y., U.S.A., 1975), to be published.

(3) L. M. Hogan, R. W. Kraft and F. D. Lemkey, in Advances in Materials Research, edited by H. Herman (Wiley, N.Y., 1971), p. 129.

(4) E. R. Thompson and F. D. Lemkey, in Composite Materials, 4, edited by L. J. Broutman and R. H. Krock (Academic Press, N.Y., 1974), p. 101-157.

(5) F. D. Lemkey and G. McCarthy, NASA Report CR-134 678, February 1975.

(6) E. R. Thompson and F. D. Lemkey, Trans ASM, 62, pp. 140-154 (1969).

(7) H. Bibring, J. P. Trottier, M. Rabinovitch and G. Seibel, Mem. Sc. Rev. Met., 68, 23-41 (1971).

(8) H. Bibring, G. Seibel and M. Rabinovitch, Mem. Sc. Rev. Met., 69, 341-358 (1972).

(9) J. L. Walter and H. E. Cline, Met. Trans., 4, 1775 (1973).

(10) E. R. Buchanan and L. A. Tarshis, Met. Trans., 4, 1895 (1973).

(11) F. Mollard, B. Lux and J. C. Hubert, Z. Metallkunde, 65 (1974).

(12) F. D. Lemkey and E. R. Thompson, Met. Trans., 1, 2799 (1970).

(13) P. R. Sahm and M. Lorenz, J. Mat. Sc., 7, pp. 793-806 (1972)

(14) F. D. Lemkey and E. R. Thompson, Met. Trans., 2, 1537 (1971).

(15) W. Köster and S. Kabermann, Archiv für Eisenhüttenwesen, 10, 627 (1955).

(16) J. van den Boomgard and L. R. Wolff, J. Crystal Growth, 15, 11 (1972).

(17) D. Jaffrey and S. Marich, Met. Trans., 3, 551 (1972).

(18) J. J. Hanak, J. of Mat. Sc., 5, 964 (1970).

(19) L. Kaufman and H. Bernstein, Computer Calculations of Phase Diagrams (Academic Press, N.Y., 1970).

(20) H. Gaye and C.H.P. Lupis, Met. Trans., 6, 1049 (1975).

(21) G. B. Stringfellow, J. of Crystal Growth, 27, 21-34 (1974).

(22) V. T. Mager and C. Petzow, Z. Metallkunde, 63, 702 (1972).

(23) E. Blank, AGARD Conference Proceedings 156, (Harford House, London, 1974), p. 81.

(24) Alloy Phase Equilibria, A. Prince (Elsevier, Amsterdam, 1960).

(25) J. C. Hubert, M. S. Thesis (University of Montreal, 1968).

(26) A. S. Yue and J. B. Clark, Trans. AIME, 221, 383 (1961).

(27) R. S. Mints, G. F. Belyayeva and Y. S. Malkov, Russian Met., 2, 96 (1967).

(28) L. Kaufman and H. Nesor, NASA Report CR-134 608 (NASA Lewis Research Center, January, 1974).

(29) V. N. Svechnikov and V. M. Pan, Summaries of Scientific Work of the Institute of Metal Physics of the Academy of Sciences of Ukranian SSR, 8, 46-57 (1962).

(30) L. Kaufman and H. Nesor, Reference 1, Volume III, p. 21.

(31) E. Rudy, Ternary Phase Equilibria in Transition Metals B-C-Si Systems (AFML, Wright Patterson AFB, Ohio, 1969).

(32) E. Rudy, F. Benesovsky and L. Toth, Z. Metallkunde, 54, 345 (1963).

(33) H. Sprenger, H. Richter and J. J. Nickl, to be published in Proceedings of the Second Conference on In-Situ Composites.

APPENDIX A

LIST OF ALLOY COMPOSITIONS PREPARED IN THE PRESENT ALLOY SCREENING STUDY

Alloy	Compositions (wt%)	Eutectic observed
NICKEL-BASE		
Ni-Al-Ti	80.5- 6 -13.5	yes
	79 - 6 -15	yes
	75 - 6 -19	yes
Ni-Al-Zr	82 -12 - 6	yes
	75 -16 - 9	yes
Ni-Si-Ti	76 - 6 -18	no
	70 - 6 -24	no
	70 -12 -18	no
Ni-Si-V	70 -26 - 4	yes
Ni-Cr-Si	59 -32 - 9	no
	55 -37 - 8	no
	53 -38 -15	no
Ni-Cr-Ti	60 -20 -20	yes
	53.7-29 -17.3	yes
	54.2-4.6-41.2	eutectic composition
Ni-Cr-Hf	60.8-30.3- 8.9	yes
	65 -25 -10	yes
	55 -30 -15	yes
Ni-Cr-Nb	44.1-42 -13.9	yes
	60 -26 -14	yes
	55 -25 -20	yes
Ni-Nb-B-C	85 -13 - 1.1-0.9	yes
	80 -18 - 1.2-0.8	yes
Ni-Mo-B-C	65 -31 - 2.1-1.9	yes
	68 -28 - 2.1-1.9	yes
NI(Cu)-Mo-B-C	63 - 5 -28-2.1-1.9	yes
Co-BASE		
Co-Al-Zr	80.5-11 - 8.5	yes
	82.2-12 - 5.8	yes
Co-Al-Nb	74.8- 2.7-22.5	yes
	75.8- 2.5-21.7	yes
	73.7- 3.2-23.1	eutectic composition
Co-Al-Ta	64.2-31 - 4.8	yes
	67.8-28.7- 3.5	yes
Co-C-Zr	85 - 3 -12	no
	81 - 9 -12	no
	73 - 9 -18	no
Co-Si-Ti	60 -10 -30	yes
	70 - 7.5-22.5	yes
	75 - 7 -18	yes
	80 - 5 -15	yes
Co-Si-Zr	78 - 4.6-17.4	yes
	80 - 5 -15	yes
	82.5- 4.5-13	eutectic composition
Co-Si-V	66 - 4 -30	yes
	70 - 4 -26	yes
Co-Cr-Si	55 -35 -10	yes
	70 -25 - 5	yes
	55 -40 - 5	yes
Co-Cr-Nb	55 -19.5-25.5	yes
	65 -17 -28	yes
Co-Cr-Mo	65 - 7 -28	yes
	63 - 7 -30	yes
	60 -12 -28	eutectic composition

APPENDIX A (Continued)

Alloy	Composition (wt%)	Eutectic observed
Fe-BASE		
Fe-Si-Ti	60-15 -25	yes
	68-10 -22	yes
Fe-Si-Zr	70-10 -20	yes
	75- 5 -20	yes
Fe-Si-V	63-30 - 7	yes
	65-29 - 6	yes
Fe-Cr-Ti	60- 5 -35	no
	70-15 -25	no
	80- 5 -15	no
Fe-Cr-Zr	71- 9 -20	no
	65-15 -20	no
	65- 9 -26	no
Fe-Cr-Ta	65-21.7-13.3	yes
	60.25 -15	yes

APPENDIX B

SUMMARY OF OXIDATION BEHAVIOR AT 1150°C IN 100 mm Hg OXYGEN

Alloy Number	Alloy Composition	Oxidation Rate $\dot{k}_p$ ($g^2 cm^{-4} sec^{-1}$)	Remarks
A	Co-35Cr	9.75×10^{-11}	Forms continuous, protective Cr_2O_3 film.
B	Co-10Cr	1.11×10^{-7}	Forms nonprotective, Co-rich scale.
C	Ni-30Cr	2.68×10^{-11}	Forms continuous, protective Cr_2O_3 film.
BGL-1	Co-28Mo-12Cr	1.29×10^{-8}	Mostly uniform attack but some evidence of accelerated local attack. Nonadherent scale.
BGL-2	Co-23.1Nb-3.2Al	Not parabolic, rate similar to Alloy B.	Uniform attack, little preferential penetration.
BGL-3	Ni-25Cr-20Nb	Not parabolic, rate similar to Alloy BGL-2	Extensive internal attack, suggestive of molten phase.
BGL-4	Ni-42.1Ti-4.6Cr	Not parabolic, slower than BGL-1	Alloy not homogeneous. Where single phase (Cr-rich?), protective behavior. Where eutectic present, rapid, uneven attack.
BGL-5	Co-17.4Zr-4.6Si	7.74×10^{-9}	Alloy not homogeneous where single phase--V. uniform but rapid attack. Where eutectic present, preferential but not catastrophic attack of eutectic. All scale adhered.
BGL-6	Co-30Ti-10Si	2.42×10^{-8}	Relatively uniform, but rapid attack. Alloy contains porosity. Complex oxidation products.
BGL-7	Co-40Cr-5Si	2.47×10^{-11}	Uniform, thin scale, not adherent, locally extensive amount of grain boundary penetration.
BGL-8	Ni-37Cr-8Si	8.94×10^{-11}	Exceptionally nonuniform attack, deep grain boundary penetration. Possibly surface liquid phase formed?
BGL-9	Co-18.5Cr-11Nb	6.47×10^{-8}	V. uniform attack, no preferential oxidation
BGL-10	Co-13Zr-4.5Si	$\sim 1.2 \times 10^{-7}$	Relatively uniform attack.
BGL-11	Ni-6Al-19Ti	$\sim 3.9 \times 10^{-8}$	Uniform but extensive internal oxidation
BGL-12	Ni-12Al-6Zr	4.65×10^{-9}	Internal oxidation, severe in places
BGL-13	Ni-30.3Cr-8.9Hf	5.71×10^{-10}	Scale not adherent. Internal oxidation of Hf-rich phase leading to deep penetration.
BGL-14	Co-12.1Al-5.7Zr	$\sim 2 \times 10^{-8}$	Alloy not homogeneous. Over most of alloy scale appears to be Al_2O_3-rich. Weight gain due to rapid oxidation of Zr-rich phase.
BGL-15	Fe-10Si-22Ti	$\sim 1.4 \times 10^{-8}$	External scale spalled. Relatively uniform internal oxidation with formation of a uniform, brittle denuded layer in alloy.
BGL-16	Fe-20Zr-5Si	-	Catastrophic oxidation, localized rapid penetration of oxide, possibly associated with alloy inhomogeneities.
BGL-17	Fe-21.7Cr-13.3Ta	-	Alloy not homogeneous. One phase oxidized slowly (Fe-Cr), other oxidized rapidly and completely, or possibly melted.
BGL-18	Ni-2.5Al-19.7Nb-6Cr	-	Not parabolic, slower than Ni-30Cr (which forms protective Cr_2O_3 scale), extensive scale spallation and limited preferential attack of aligned phase.
BGL-19	Co-20TaC-15Cr-8.5Ni-6W	1.63×10^{-8}	Uniform but nonadherent scale, very little preferential attack of alloy.

DISTRIBUTION LIST
(One copy unless otherwise noted)

(3 copies plus balance after distribution)
Naval Air Systems Command
(AIR-52031B)
Department of the Navy
Washington, D.C. 20361

(7 copies for internal distribution by AIR-954, as follows: AIR-954 (2 copies), AIR-536B1 (1 copy), AIR-330A (1 copy), AIR-330B (1 copy), AIR-5361A (1 copy), AIR-5362A (1 copy))
Naval Air Systems Command
(AIR-954)
Department of the Navy
Washington, D.C. 20361

Commander
Naval Air Development Center
(Code 30232)
Warminster, Pennsylvania 18974

Naval Air Turbine Test Station
Attn: R. Lister (AT-1P)
1440 Parkway Avenue
Trenton, New Jersey 08628

Commander Naval Weapons Center
(Code 5516)
China Lake, California 93555

Naval Ships Engineering Center
(Code 6146)
Department of the Navy
Center Building
Prince George's Center
Hyattsville, Maryland 20782

U. S. Naval Sea Systems Commands
Code 035
Department of the Navy
Washington, D. C. 20360

Naval Ships Research & Development
Center
(Code 2812)
Annapolis, Maryland 21402

Commander, Naval Ordnance Laboratory
(Metallurgy Division)
White Oak
Silver Spring, Maryland 20910

(2 copies)
Director, Naval Research Laboratory
(Code 6330 - 1 copy)
(Code 6306 - 1 copy)
Washington, D.C. 20390

Office of Naval Research
The Metallurgy Program, Code 471
Arlington, Virginia 22217

(2 copies)
Director
Army Materials & Mechanics Research
Center
A. Gorum (1 copy)
P. Ahearn (1 copy)
Watertown, Massachusetts 02172

Commander, Army Material Command
Attn: AMCRD-TC
50001 Eisenhower Avenue
Alexandria, Virginia 22304

Commander, Army Munitions Command
Frankford Arsenal
Attn: D. Kleppinger
Pitman Dunn Lab.
Philadelphia, Pennsylvania 19137

(3 copies)
Air Force Materials Laboratory
(Code LLS - 1 copy)
(Code LLC - 1 copy)
(Code LT - 1 copy)
Wright-Patterson Air Force Base
Ohio 45433

National Aeronautics & Space
Administration
(Code EWM)
Washington, D. C. 20546

(3 copies)
National Aeronautics & Space
Administration
Lewis Research Center
G. M. Ault (1 copy)
H. P. Probst (1 copy)
Dr. R. L. Ashbrook (1 copy)
21000 Brookpark Road
Cleveland, Ohio 44135

Distribution List (Cont'd)

Atomic Energy Commission
Division of Reactor Development
(A Van Echo)
Washington, D. C. 20545

Metals & Ceramics Information Center
Battelle Memorial Institute
505 King Avenue
Columbus, Ohio 43201

The Johns Hopkins University
Applied Physics Laboratory
Attn: Maynard L. Hill
8621 Georgia Avenue
Silver Spring, Maryland 20910

AVCO RAD
201 Lowell Street
Wilmington, Massachusetts 01887

IIT Research Institute
Attn: Dr. M.A.H. Howes
10 West 35th Street
Chicago, Illinois 60616

Detroit Diesel Allison Division
General Motors Corporation
Materials Laboratories
Indianapolis, Indiana 46206

United Aircraft Company
Pratt & Whitney Aircraft Division
East Hartford, Connecticut 06108

United Technologies Research Center
East Hartford, Connecticut 06108

Lockheed Aircraft Company
Attn: Dr. M. I. Jacobson
ORGN 80-72
Building 182
P. O. Box 504
Sunnyvale, California 91088

Airesearch Division
Garrett Corporation
Phoenix, Arizona 85001

Lycoming Division
AVCO Corporation
Stratford, Connecticut 06497

Curtis Wright Company
Wright Aeronautical Division
Wood-Ridge, New Jersey 07075

Bell Aerosystems Company
Technical Library
P. O. Box 1
Buffalo, New York 14240

General Electric Company
Aircraft Engine Group
Materials & Processes Technology Labs.
Evendale, Ohio 45215

Solar
Attn: Dr. A. Metcalfe
2200 Pacific Highway
San Diego, California 92112

Teledyne CAE
1330 Laskey Road
Toledo, Ohio 43601

Stellite Division
Cabot Company
Technical Library
P. O. Box 746
Kokomo, Indiana 46901

Materials Research Company
Attn: Dr. S. Weinig
Orangeburg, New York 10962

Artech Company
Attn: Mr. Henry Hahn
2816 Fallfax Drive
Falls Church, Virginia 22042

Dr. Merton C. Flemings
Room 35-316
Massachusetts Inst. of Technology
Cambridge, Massachusetts 02139

Professor R. Wayne Kraft
Department of Metallurgy & Materials
Science
Lehigh University
Bethlehem, Pennsylvania 18015

Distribution List (Cont'd)

Professor Nicholas J. Grant
Department of Metallurgy & Materials
Sciences
Massachusetts Inst. of Technology
Cambridge, Massachusetts 02139

Dr. Kenneth A. Jackson
Member of the Staff
Bell Telephone Laboratories Inc.
600 Mountain Avenue
Murry Hill, New Jersey 07974

National Academy of Sciences
Materials Advisory Board
Attn: Dr. J. Lane
Washington, D. C. 20418

Reynolds Metal Company
Attn: Technical Library
Reynolds Metals Bldg.
Richmond, Virginia 23218

P. R. Mallory & Company, Inc.
Attn: Technical Librarian
3029 East Washington Street
Indianapolis, Indiana 46206

Midwest Research Institute
425 Volker Boulevard
Kansas City, Missouri 64110

Aluminum Company of America
Attn: Mr. G. B. Barthold
1200 Ring Bldg.
Washington, D.C. 20036

Professor Alan Lawley
Head, Department of Metallurgical
Engineering
Drexel University
32nd & Chestnut Streets
Philadelphia, Pennsylvania 19104

Dr. A. I. Mlavsky
Tyco Laboratories, Inc.
16 Hickory Drive
Waltham, Massachusetts 02145

Whittaker Company
Nuclear Metals Division
Attn: Dr. A. S. Bufferd
West Concord, Massachusetts 01718

University of California
Lawrence Radiation Laboratory
Attn: Technical Information Division
Livermore, California 94550

TRW Equipment Laboratories
Attn: Mr. J. A. Alexander
23555 Euclid Avenue
Cleveland, Ohio 44117

(3 copies)
General Electric Company
Corporate Research & Development
M. G. Benz (1 copy)
Dr. James D. Livingston (1 copy)
R. Charles (1 copy)
P. O. Box 8
Schenectady, New York 12301

(~~12~~ 5 copies)
Defense Documentation Center
Cameron Station
Alexandria, Virginia 22314
Via: Commander
Naval Air Systems Command
(AIR-50174)
Department of the Navy
Washington, D. C. 20361

(1 copy)
NASA
Scientific & Technical Information
Facility
P. O. Box 33
College Park, Maryland 20740

Grumman Aerospace Corporation
Bethpage, New York 11714

DCASO-Columbus (ltr. only)